われわれが副作用予測マーカー開発のために用いた血液はゲムシタビン治療前に採血されたものであるため，このデータを予後予測の観点から臨床情報を見直し，予後の良否を反映するピークを探索すれば，ゲムシタビン治療による予後を予測するマーカーが開発できる可能性がある．そのため前述の副作用予測マーカー開発のためにLC-MS測定した症例のなかから，生存率の両極端な症例群（長期生存例：31例，早期死亡例：29例）を選別し，2DICALで解析した．両群間で差の大きかったペプチドピークを選別しそのアミノ酸配列を決定したところ，α1アンチトリプシンとα1アンチキモトリプシンが同定された（図3B）．

❖検証過程

RPPAを用いてα1アンチトリプシンとα1アンチキモトリプシンの検証を行った．ゲムシタビン治療を受けた膵がん患者304症例の治療前血漿（252例），または血清（52例）を500～4,000倍まで4段階に希釈してガラス基板にスポットし，抗α1アンチトリプシン抗体と抗α1アンチキモトリプシン抗体で反応させた．RPPA測定でα1アンチトリプシンの反応強度の低い124例の生存日数中央値は327日であったのに対し，反応強度の高い180例では生存日数中央値が201日と短く，ゲムシタビン治療開始時にα1アンチトリプシンの高い症例では有意に予後が不良であることが示された．α1アンチキモトリプシンも同様にその反応強度の違いで生存日数に有意差が認められたが，他の臨床情報とともに多変量解析を行うと，α1アンチトリプシン，アルカリホスファターゼ，白血球数，PS（performance status）が生存にかかわる因子として選別された[8]．

文献

1）Ono, M. et al. : Mol. Cell. Proteomics, 5 : 1338-1347, 2006
2）Gygi, S. P. et al. : Nat. Biotechnol., 17 : 994-999, 1999
3）DeSouza, L. et al. : J. Proteome Res., 4 : 377-386, 2005
4）Li, X. J. et al. : Anal. Chem., 76 : 3856-3860, 2004
5）Ishihama, Y. et al. : Mol. Cell. Proteomics, 4 : 1265-1272, 2005
6）Ono, M. et al. : J. Biol. Chem., 284 : 29041-29049, 2009
7）尾野雅哉：細胞工学別冊　明日を拓く新次元プロテオミクス（中山敬一，松本雅記/監），pp 122-130, 秀潤社，2009
8）Matsubara, J. et al. : Mol. Cell. Proteomics, 9 : 695-704, 2010
9）尾野雅哉：実験医学増刊　分子レベルから迫る癌診断研究～臨床応用への挑戦～（中村祐輔/監），pp124-132, 羊土社，2007
10）尾野雅哉，他：Cancer Frontier, 10 : 14-20, 2008
11）Honda, K. et al. : Cancer Res., 65 : 10613-10622, 2005
12）江川新一，他：膵臓，23 : 105-123, 2008
13）Sakaguchi, N. et al. : J. Immunol., 174 : 4485-4494, 2005
14）Matsubara, J. et al. : J. Clin. Oncol., 27 : 2261-2268, 2009
15）Matsubara, J. et al. : Eur. J. Clin. Med. Oncol., 1 : 1-6, 2009

2 腫瘍マーカー温故知新

尾野雅哉

腫瘍マーカーは，その歴史から見れば基礎医学が臨床医学に貢献した業績の１つである．CEA, Ca19-9 は癌特異（関連）抗原として発見されたが，臨床現場では採血という低侵襲で簡便に癌の存在を知ることができる便利なマーカーとして受け入れられた．現在，医学研究技術の急速な進歩に伴い，高感度かつ特異的に癌を認識し，癌の早期に存在診断を可能にする古典的な意味合いでの新しい腫瘍マーカーだけでなく，鑑別診断，転移再発予測，治療効果予測など，様々な臨床現場で役に立つ腫瘍マーカーの開発への期待も高まっている．本稿では，腫瘍マーカー開発を“温故”し，“知新”に向けて，その現況と未来を概説する．

key word　腫瘍マーカー，網羅的解析，プロテオミクス，2DICAL

Ⅰ．腫瘍マーカーを“温故”する

1．腫瘍マーカーの歴史

腫瘍マーカーは，筆者が医師となった1980年代にはすでに一般的に使われていたが，有名な腫瘍マーカーであるCEAやCa19-9は当時，癌特異抗原，癌関連抗原とも呼ばれていた．腫瘍マーカーを“温故”すると，Rudolf Virchowが築いた近代病理学で，癌が細胞の異常であることを認識し，その異常を来す本質を探し求めた先人たちの歴史にたどりつき，それは正常細胞にはなく癌細胞にのみある物質（cancer aberration）を探し出すという今なお続く歴史の始まりをも知ることができる．数え切れぬ仕事がなされた中で，癌を免疫して得られた抗血清（抗体）による研究が腫瘍マーカーへの道を拓いた[1]．

消化器癌の腫瘍マーカーとして用いられるCEAはヒト大腸癌抽出物をウサギに免疫した抗血清で認識される，癌（cancer）と胎児胚（embryo）に特異的な抗原（carcinoembryonic antigen）として1965年に発表された[2, 3]．その後，Thomsonら[4]により血中CEA濃度の測定法が開発され，臨床の場で血中CEAが測定されるようになった．この時点ではCEAは抗体が認識するある物質であり，構造は不明であったが，癌で高値を示すCEAは血液で癌の診断ができる可能性を示し，当時の医師には驚きをもって受け入れられたことは想像に難くないことである．代表的な腫瘍マーカーであるCa19-9も，大腸癌細胞株をネズミに免疫した抗体で認識される大腸癌に特異的に発現する抗原として1979年に発表された[5]．その後，この抗原は種々の消化器癌，特に膵臓癌に発現することが明らかとなり，構造もSialyl Le^{a}という糖鎖[6]であることも判明した．しかし，Ca19-9がSialyl Le^{a}という構造であることを筆者が認識したのは臨床の場で用い始めてからずっと後のことであった．

このようにCEA, Ca19-9は癌特異抗原として研究室（Bench）で発見されたが，採血という低侵襲で簡便に癌の存在を知ることができる便利なマーカーとして臨床（Bed）に受け入れられた．詳細な機能や構造が不明でも，臨床の現場で測られ，簡便な方法で癌を把握できる“腫瘍マーカー”の地位が確立した．

2．腫瘍マーカーとは何か

腫瘍マーカーはバイオマーカーの1つであり，バイオマーカーは“a characteristic that is objectively measured and evaluated as an indicator of normal biologic processes, pathogenic processes, or pharmacologic responses to a therapeutic intervention (NIH study group)”[7]と定義されるように，生理的，病理的，薬理的な変化に対応する計測可能な客観的な指標となる性格を有するものである．上記の定義に従えば，癌が作り出すもの以外に，癌に対する宿主の反応も計測可能な客観的な指標であれば腫瘍マーカーになりうる．生体内に癌ができれば，それに対して何らかの反応を起こしているのはCancer Survey[8]という概念で捉えられている．また，癌患者には癌に対する自己抗体が存在するのは多くの文献から明らかである[9, 10]．癌から分泌される物質よりこのような生体反応に起因する物質のほうが，癌が微小な場合には量的に多く血液中に現れ，より

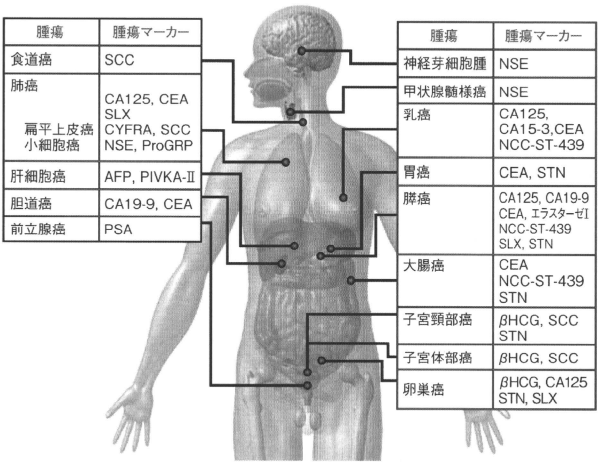

■図1　臓器別腫瘍マーカーの一覧
AFP；α-フェトプロテイン，βHCG；ヒト絨毛性ゴナドトロピン，CA125；MUC16，CA19-9；シアリルルイスA（糖鎖），CEA；癌胎児性抗原，CYFRA；サイトケラチン19，NCC-ST-439；シアリルルイスX（糖鎖），NSE；神経特異エノラーゼ，PIVKA-Ⅱ；protein induced by vitamin K absence or antagonist-Ⅱ，ProGRP；ガストリン放出ペプチド前駆体，PSA；前立腺特異抗原，SCC；扁平上皮癌関連抗原，SLX；シアリルルイスX（糖鎖），STN；シアリルTn（糖鎖）．
国立がん研究センターがん対策情報センターHP（http://ganjoho.jp/public/dia_tre/diagnosis/tumor_marker.html）より改変．

感度の高いマーカーとなりうる可能性もある．

癌の臨床には，癌の発見のみではなく，鑑別診断，治療法の選択，治療中，経過観察中の患者支援など様々な場面がある．臨床医はあらゆる情報を総合的に判断して正しい道を選ぶ努力を常に行っているが，その決定が難しいときには何らかの新しい情報を必要とする．そのような場面で病態把握に役立つのであれば，腫瘍の臨床に関わるマーカーとして腫瘍マーカーの意義が認められる．乳癌のトラスツズマブ（ハーセプチン）治療にあたってHER2発現量を測定することは当然のことではあるが，治療法選択における腫瘍マーカーの具体例とも言える．

癌細胞に由来する物質のみではなく，癌の存在による宿主の変化も腫瘍マーカーとして捉えることにより，癌の診断だけでなく，より有効な治療にも結びつくものとなる．腫瘍マーカーに期待されるものは，CEAやCa19-9が開発された時代より大きく拡がってきたと言える．

3.現在用いられている腫瘍マーカー

国立がん研究センターのホームページより腫瘍マーカーの一覧を転載した（図1）．これらは，癌の進展に伴って血中で高値を示してくるもので，癌細胞に由来する物質である．多くは癌細胞を免疫する方法で選び出されてきたもので，本体が糖鎖であるものも多く含まれている．これらの腫瘍マーカーが開発された当初は，腫瘍特異抗原として腫瘍のみを認識できるものと注目されたが，その後の研究により腫瘍以外の正常組織にも存在することが確認され，腫瘍関連抗原と呼ばれるようになった．

これらの腫瘍マーカーは，他の疾患でも上昇する場合があること（特異度）と，癌が存在しても高値を示さない場合があること（感度）が問題点として挙げられる．これは腫瘍マーカーが高値であるからといって癌が確定できず，低値であるからといって癌を否定できないことを意味し，運用にあたっての不明瞭さが常に指摘されている．もちろんこのような状況で正しい判断をすることが臨床医の腕の見せ所であるが，判断ミスを最小限に抑えるためにも，より特異度，感度の高い新規腫瘍マーカーや腫瘍マーカーの組み合わせが求められている．

Ⅱ．腫瘍マーカーの“知新”

1.解析技術の進歩

腫瘍マーカーの開発は，正常にはなく癌にのみある物質を探し出すことであるが，基本的には多くの情報から適切なものを選び出す網羅的解析手法（comprehensive analysis）がとられてきた．抗体による腫瘍マーカーの開発も，癌細胞を動物に免疫して得られる非常に多くの抗体の中から，癌を選

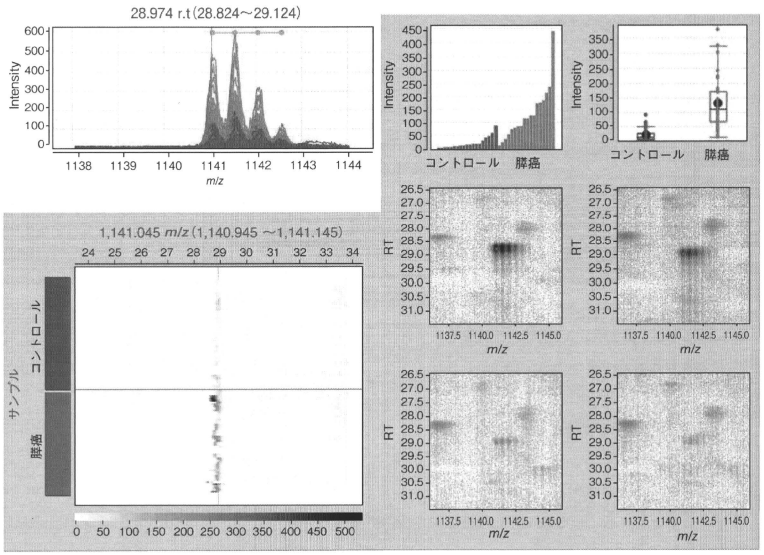

■図2　2DICALによる膵癌の解析結果(文献17)より改変)
質量分析計のデータを質量電荷比(*m/z*)，保持時間(RT)，ピーク強度(Intensity)，サンプル(Sample)の4つの変数で表すことにより，多数サンプル間で同一ピーク同士の比較が正確に行えるようになった．膵癌患者血漿(赤)と健常者血漿(青)の比較で有意に差のあった(*m/z*，RT)＝(1141.0, 28.9)のピークを様々な組み合わせの座標軸で示した二次元画像を示す．

択的に認識する抗体を選び出す作業であった．分子生物学の解析手法が発展し，癌細胞に特徴的な遺伝子変化を網羅的に調べる時代が訪れると，数多くの遺伝子の中から，癌になる遺伝子，転移を起こす遺伝子，予後と関係する遺伝子などが選び出された．いずれもその時代の最先端の解析技術が用いられており，技術の進歩は新しい腫瘍マーカーを生み出す原動力となってきた．

現在の最先端解析技術として，DNAの高速シークエンサーが注目を浴びているが，ポストゲノムの解析技術としてプロテオミクスも期待されている分野である[11]．プロテオミクスに用いられる技術の中で，質量分析計の進歩は目を見張るものがある．1台が数千万円から1億円以上する高価な計測機器であるため対費用効果が高く，国家戦略，企業戦略として重要視されているため，質量分析計開発メーカー間での競争は激しく，解析能力が年々伸びていることを実感する．プロテオミクスにおいては，遺伝子解析のように増幅することができないため，実際の量を計測する技術が求められる．このためには，どれだけ微量なものを測れるか(感度)はもちろん重要であるが，非常に少ない量の物質を多量に存在する物質の中から見いだす能力(ダイナミックレンジ)がきわめて重要となる．血液では最も豊富なアルブミンとサイトカインなどごく微量な物質との濃度差は10^{12}あるとされており，すべてを見るには10^{12}のダイナミックレンジを必要とする．最新の機器でもダイナミックレンジは10^{5}程度であるが，技術の進歩はその限界を克服する可能性を感じさせる．

2.水酸化プロリンα-フィブリノーゲン

筆者らはプロテオミクスの最新技術として，2DICAL(2 dimensional image converted analysis of liquid chromatography and mass spectrometry)を開発した．詳細は別誌に譲るが[12), 13)]，質量分析計で得られるデータを二次元電気泳動ゲルのような二次元画像に変換して解析する

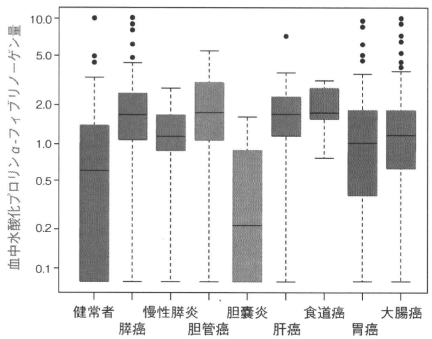

■図3 水酸化プロリンα-フィブリノーゲンの種々の癌および良性疾患における血中濃度分布(文献17)より改変)
水酸化プロリンα-フィブリノーゲンは種々の癌および慢性膵炎で上昇が見られる．また，健常者群でも高値を示す例が存在している．

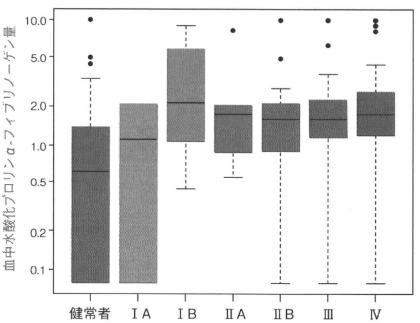

■図4 水酸化プロリンα-フィブリノーゲンの膵癌ステージ別の血中濃度分布(文献17)より改変)
水酸化プロリンα-フィブリノーゲンは膵癌ステージⅠBから上昇が見られる．

システムである．このシステムにより，子宮体癌腫瘍マーカー[14]，膵癌化学療法による副作用予測マーカー[15]，膵癌化学療法後の予後予測マーカー[16]などの新規腫瘍マーカーの開発に成功しているが，それらの中で血中水酸化プロリンα-フィブリノーゲンについて解説する[17]．

血漿膵癌腫瘍マーカーを探索するために，膵癌患者血漿および健常者血漿それぞれ43症例を2DICALで解析し，両群間で有意差のあるピークを選出した(図2)．精密質量分析計で解析を行い，このピークがプロリン残基に酸素1原子が付加したα-フィブリノーゲンのペプチド断片であることを証明した．プロリン残基の酸素付加で安定した構造は水酸化プロリンであるため，さらに，4-水酸化プロリンに置換した合成ペプチドに対する抗体を作製し，水酸化プロリンα-フィブリノーゲンが膵癌患者血漿で上昇していることを確認した．

研究室で見いだされた物質が腫瘍マーカーとして認められるためには多数例での検証が必須である[18]．筆者らは水酸化プロリンα-フィブリノーゲン測定用ELISAを作製し，多施設共同研究で収集した686例の血中量を測定したところ，健常者に比べ各種の癌および慢性膵炎で有意に上昇していることが確認された(図3)．このように，特定の癌の腫瘍マーカーとして開発を目指したものが，検証の段階で他の癌や疾患にも陽性に反応することがあるのは今までの腫瘍マーカーの開発からも示されており，新規の腫瘍マーカーは多数例の検証後に運用法を考慮していかなければならないことを示すものである．

水酸化プロリンα-フィブリノーゲンに関しては，膵癌の早期段階から上昇すること(図4)や多くの癌で高値を示すことから，膵癌の早期診断や癌検診への応用が期待される．特に，研究に参加する健常者集団は健康診断受診者集団と重なるため，健常者に見られる高値例は注目すべき結果である．また，長年研究されたフィブリノーゲンにこのような構造が存在していることは初めて発見された事実であり，その生物学的意義は今後検討していかなければならない課題である．現時点の解析では，水酸化プロリンα-フィブリノーゲンは膵癌では産生されておらず，肝組織で産生されていること，P4HA(prolyl 4-hydroxylase A)が合成に関与していることが確認されている．

3. 今後の展開

腫瘍マーカーとは，臨床の場で役立つものである．腫瘍マーカーの開発はその歴史的な背景を鑑みてもトランスレーショナルリサーチのわかりやすい一例であり，臨床と基礎が密接に関連しながら，どのような腫瘍マーカーを開発していくかを議論することが最も重要である．

癌の存在診断，鑑別診断，転移再発予測，治療有効性の判定においても，腫瘍マーカーは感度，特異度ともに100%であるものが理想である．しかし，癌は様々に異なった性質を持っており，その癌を持つ宿主にも様々な違いがある．1つ

の因子のみですべてを説明できるほど単純でないことは，癌に関わってきたものには周知のことである．例えば，同じ遺伝型でも栄養状態が違えば癌に対する反応も違ってくる．癌の性質と担癌患者の総体に関する情報を集約し，画像診断を含め，より有効な個別化医療ができるように腫瘍マーカーを運用することが今後の課題である．

現在の技術は様々な物質を網羅的に解析することが可能となってきており，すべての分子で生命を説明する真の分子生物学が急速に進んでいる．今後はタンパク質，遺伝子，糖鎖だけでなく，脂質や代謝産物など生命を構成するあらゆる分子から腫瘍マーカーが開発される可能性がある．また，質量分析計のMRM/SRM (multiple reaction monitoring/selective reaction monitoring) 技術が進めば，一度にすべての腫瘍マーカーが測定できるときが訪れる可能性もある．腫瘍マーカーの開発と効率のよい運用法の開発は，癌の診断治療の効率化とともに，医療コスト削減という社会経済へも深く貢献することになると予測される．

おわりに

筆者が学生時代に受けた発生学の講義は，発生の途中ではいろいろな細胞が体中を動いているといったぼんやりとした印象しかないのだが，いまだに深く記憶に残っている．そのときの教科書であるラングマンの「人体発生学」[19]を見ると，消化管に存在する器官神経叢は知覚性神経節の細胞が移動したものだと記載されている．転移とはある場所を離れて他の場所で細胞が増殖することであるが，その能力は正常細胞にも備わっているもののようである．ただし，癌細胞と正常細胞とでは制御が効くか，効かないかという点で違っている．転移のメカニズムは非常に複雑なものであるが，それを制御するメカニズムやそれを動かす物質は必ず存在しているはずである[20), 21)]．我々が生命を分子や原子という目で見るようになったのは，長い生命の歴史から見れば，ほんの少し前のことであり，これから進歩していく技術によってその解を見つけ出すことができるに違いない．転移を制御することは，癌を制圧することであり，それを可能ならしめるためには，癌に関わるあらゆる知恵を結晶させていかなければならない．

PROFILE

尾野雅哉

■ 独立行政法人 国立がん研究センター研究所 化学療法部 室長
■ E-mail：masono@ncc.go.jp

1983年東京大学医学部卒業．東京大学第一外科入局．1992～1994年，国立がんセンターがん専門修練医．1994年より東京大学第一外科助手．1997～2000年ワシントン大学留学（箱守仙一郎教授に師事）．自治医科大学消化器一般外科講師を経て，2003年より現職．

文献

1) Hakomori S: Adv Cancer Res (1989) 52: 257-331
2) Gold P, et al: J Exp Med (1965) 121: 439-462
3) Gold P, et al: J Exp Med (1965) 122: 467-481
4) Thomson DM, et al: Proc Natl Acad Sci USA (1969) 64: 161-167
5) Koprowski H, et al: Somatic Cell Genet (1979) 5: 957-971
6) Magnani JL, et al: J Biol Chem (1982) 257: 14365-14369
7) NIH: Biomarkers Knowledge System Meeting Report September 8, 2000
8) Dunn GP, et al: Nat Immunol (2002) 3: 991-998
9) Soussi T: Cancer Res (2000) 60: 1777-1788
10) Wang X, et al: N Engl J Med (2005) 353: 1224-1235
11) 尾野雅哉ら：実験医学 (2007) 25: 2714-2722
12) Ono M, et al: Mol Cell Proteomics (2006) 5: 1338-1347
13) 尾野雅哉ら：2DCALを用いた疾患バイオマーカー探索（中山敬一ら 監修，明日を拓く新次元プロテオミクス，秀潤社）：pp.122-130, 2009
14) Negishi A, et al: Cancer Sci (2009) 100: 514-519
15) Matsubara J, et al: J Clin Oncol (2009) 27: 2261-2268
16) Matsubara J, et al: Mol Cell Proteomics (2010) 9: 695-704
17) Ono M, et al: J Biol Chem (2009) 284: 29041-29049
18) 尾野雅哉ら：Cancer Frontier (2008) 10: 14-20
19) Langman J: 人体発生学 正常と異常，第3版（沢野十蔵 訳，医歯薬出版）：1976
20) Ono M, et al: Cancer (1996) 78: 1179-1186
21) Ono M, et al: Glycoconj J (2004) 20: 71-78

research articles Journal of proteome research

A Peptidomics Strategy for Discovering Endogenous Bioactive Peptides

Kazuki Sasaki,*,† Noriyuki Takahashi,‡ Mitsuo Satoh,§ Motoo Yamasaki,‡ and Naoto Minamino*,†

Department of Molecular Pharmacology, National Cerebral and Cardiovascular Center Research Institute, Suita, Osaka 565-8565, Japan, Innovative Drug Research Laboratories, Kyowa Hakko Kirin Co., Ltd., Machida, Tokyo 194-8533, Japan, and Antibody Research Laboratories, Kyowa Hakko Kirin Co., Ltd., Machida, Tokyo 194-8533, Japan

Received April 15, 2010

Peptide hormones and neuropeptides constitute an important class of naturally occurring peptides that are generated from precursor proteins by limited proteolytic processing. An important but unaddressed issue in peptidomics is to pin down novel bioactive peptides in a bulk of peptide sequences provided by tandem mass spectrometry. Here, we describe an approach to simultaneously screen for bioactive peptides and their target tissues. The principle behind this approach is to identify intact secretory peptides that have the ability to raise intracellular calcium levels. In practice, we used nanoflow liquid chromatography–tandem mass spectrometry to analyze peptides released by exocytosis from cultured cells. Peptide sequence information was utilized to deduce intact peptide forms, among which those highly conserved between species are selected and tested on an ex vivo calcium assay using tissue pieces from transgenic mice that systemically express the calcium indicator apoaequorin. The calcium assay can be applied to various cell types, including those not amenable to in vitro culture. We used this approach to identify novel bioactive neuropeptides derived from the neurosecretory protein VGF, which evoke a calcium response in the pituitary and hypothalamus.

Keywords: peptidomics • proteolytic processing • apoaequorin • secretory peptides • bioactive peptides

Introduction

Peptide hormones and neuropeptides function as cell-to-cell signaling molecules that mediate many physiological effects. The generation of these bioactive peptides involves a series of cleavage events orderly executed by specific proteases, starting with the endoproteolytic cleavage of precursor proteins to produce peptides with defined lengths.[1,2] These biosynthetic cleavages are often accompanied by post-translational modifications on specific residues, such as N-terminal acetylation and C-terminal amidation.[3] Resultant peptides, termed major processing products or "intact" peptides, are subsequently degraded and inactivated by a variety of proteases.

Peptidomics has been advocated to comprehensively study these naturally cleaved peptides that are beyond the reach of conventional proteomics.[4,5] Tandem mass spectrometry techniques enable the sequence determination of peptides present in complex mixtures for an organism whose genome sequencing nears completion. Efforts have been made to discover neuropeptides by analyzing the total peptide complement of the hypothalamus and pituitary, which are considered treasure troves of bioactive peptides.[6–9] However, despite initial enthusiasm, it has become clear that intact secretory peptides account for a relatively small proportion in a tissue peptidome. Even with known neuropeptides and peptide hormones, most of the identified peptides are N-terminally or C-terminally trimmed from intact peptides, implying that bioactive peptides, present in trace amounts, are difficult to identify in their native molecular forms.[6–9] Hence, delineating intact peptides emerges as a key factor in mass spectrometry-based peptidomic approaches to discovering bioactive peptides.

This "peptide first" approach, however, only leaves behind many peptide sequences and does not offer information about bioactivity or target tissues. One solution to the problem is to focus on post-translational modifications characteristic of known bioactive peptides, for instance C-terminal amidation.[3] Using tandem mass spectrometry, we profiled peptides secreted by cultured endocrine cells and identified novel C-terminally amidated peptides, designated NERP-1 and NERP-2.[10] Since C-terminal amidation does not guarantee that the peptides are bioactive, we were forced to conduct many hit-or-miss experiments to demonstrate that they are bioactive.[10] A more efficient method for identifying bioactive peptides would therefore be desired.

Besides the importance of investigating intact secretory peptides, we have considered the following common features

* To whom correspondence should be addressed. Department of Molecular Pharmacology, National Cerebral and Cardiovascular Center Research Institute, Fujishirodai 5-7-1, Suita, Osaka 565-8565, Japan. Phone: +81 6 6833 5004ex. 2600; Fax: +81 6 6835 5349. E-mail: ksasaki@ri.ncvc.go.jp or minamino@ri.ncvc.go.jp.

† National Cerebral and Cardiovascular Center Research Institute.

‡ Innovative Drug Research Laboratories, Kyowa Hakko Kirin Co., Ltd.

§ Antibody Research Laboratories, Kyowa Hakko Kirin Co., Ltd.

10.1021/pr1003455

Published on Web 08/04/2010

of known bioactive peptides: (1) strong interspecies homology at the amino acid level and (2) frequent use of calcium as a second messenger. In the present study, we describe an approach to screen for bioactive peptides, independent of specific modifications. The core part of this approach is to identify intact peptides released by exocytosis from cultured cells with secretory granules, followed by testing the ability of a candidate to raise intracellular calcium levels. We hypothesized that our transgenic mice systemically expressing apoaequorin, a calcium-sensitive photoprotein,[11] could be used to simultaneously screen for bioactive peptides and their target tissues. In the present study, we examined peptides derived from the neurosecretory protein VGF, the processing of which has not been elucidated, aside from the C-terminal region.[12] We used this peptidomic approach to identify two neuropeptides, hidden in the precursor sequence, that elicited a calcium transient in the pituitary and hypothalamus.

Materials and Methods

Peptide Preparation. Monolayer cultures of TT cells[13] were rinsed three times with Hanks medium (Invitrogen). Culture supernatants of the cells incubated for 15 min after stimulation with 10 μM forskolin plus 10 μM carbachol were harvested and rapidly extracted at 4C using an RP-1 solid-phase extraction cartridge (GL Sciences). Peptide fractions were obtained by HPLC on a gel filtration column (G2000SWXL, 21.5 × 300 mm, TOSOH) at 1.5 mL/min to obtain two fractions named G7−8 and G9−12, which contains peptides around 3000−7000 Da and smaller peptides (around 1000−3000 Da), respectively. Both fractions were reductive alkylated and desalted with Empore C18 cartridges (3M). The resultant samples were individually reconstituted in solvent A (10 mM ammonium formate, pH 3.8: acetonitrile (ACN) = 9:1 (v/v)) and applied to a TSK gel SP-2SW cation-exchange column (1.0 × 50 mm, TOSOH) and eluted at 50 uL/min with a gradient of 0−100% solvent B (1 M ammonium formate, pH 3.8: ACN = 9:1 (v/v)) in 30 min. Fraction G7−8 was divided into five fractions (collected every 5 min, starting 5 min after injection) and fraction G9−12 was into nine fractions (collected every 3 min, starting immediately after injection) using this cation-exchange HPLC. A total of 14 cation-exchange fractions were individually desalted with Empore C18 cartridges and analyzed by LC−MS/MS.

LC−MS/MS. NanoLC−MS/MS experiments were performed with a Chorus nanoflow system (CTC Analytics) connected to an LTQ-Orbitrap mass spectrometer (ThermoFisher Scientific) equipped with a nanoelectrospray emitter (MonoSpray C18 Nano, 100 um × 50 mm, GL Sciences).[14] Sample dissolved in 2% ACN and 0.1% formic acid was loaded via a PAL autosampler (CTC Analytics) onto an L column (Chemicals Evaluation and Research Institute, Japan) and eluted with a linear gradient from 5% ACN, 0.1% formic acid to 60% ACN, 0.1% formic acid over 40 min at 500 nL/min. A protonated ion of polycyclodimethylsiloxane with m/z 445.120025 was used for internal calibration throughout. The mass spectrometer was operated in a data-dependent mode to automatically switch between MS and MS/MS acquisitions. After survey full scan (400−1500 m/z range), five most intense ions (intensity threshold 2×10^5) were isolated for MS/MS in the linear ion trap using collision induced dissociation, with dynamic exclusion onward throughout the following scans. The resultant product ions were recorded in the Orbitrap. For each fraction, any precursor m/z (except for singly charged ions) was subjected to MS/MS and excluded thereafter if detected within a mass width of 5 ppm. Multiple identifications of the same sequence were allowed given that each identification was derived from a different precursor charge state. In addition, redundant identification of the same peptide, which was in most cases caused by distribution over multiple chromatographic fractions, was also allowed in this secretopeptidome analysis (Supplemental Table, Supporting Information).

Data Analysis and Peptide Identification. Peak picking, deisotoping, and deconvolution of MSMS spectra were performed using Mascot Distiller (ver. 2.1.1.0) with the default parameters for OrbiTrap. Peak lists were searched against IPI Human (76539 entries on March 4, 2009) using Mascot (ver. 2.2.04), with no enzyme specification. Mascot was used with monoisotopic mass selected, a precursor mass tolerance of 2 ppm, and a fragment mass tolerance of 25 mmu. Pyroglutamination and C-terminal amidation were simultaneously allowed as variable modifications. The significance threshold was the Mascot default setting of 5%. Each MSMS spectrum was checked manually to confirm or contradict the Mascot assignment. The false discovery rate for the identity threshold was in all cases 0% as estimated by using the Mascot decoy database function. Only peptides identified with a score above the Mascot identity threshold were considered in the present study.

Peptide Synthesis. All peptides were synthesized using Fmoc (*N*-(9-fluorenyl)methoxycarbonyl) strategy, purified by reversed phase HPLC (SigmaGenosys), and verified for correct synthesis by mass spectrometry and amino acid analysis.

Antibody Preparation. Cysteinyl C-terminal peptides of rat NERP-3 (CESPGPERVW) and AQEE-30 (CEHVLLHRP) were synthesized and each coupled with maleimide activated keyhole limpet hemocyanin (Pierce). Rabbits were immunized with each conjugate and antisera were characterized as described.[15]

Mass Spectrometric Characterization of VGF-Derived Peptides. Rat whole brain excluding cerebellum was extracted and condensed with a SepPak C18 cartridge as previously described.[10] Sephadex G-50 gel filtrated fractions of the rat brain extract (2.38 and 1.40 g equivalent for NERP-3 and AQEE-30, respectively) were immunoprecipitated with the antibodies and analyzed on a surface-enhanced laser desorption ionization mass spectrometer (Ciphergen) as described.[16]

Calcium Assay Using Tissues from Apoaequorin Transgenic Mice. Assays were performed as previously described with a few modifications.[11] Tissues or organs from the apoaequorin transgenic mice were cut out as 1−2 mm^3 pieces and incubated with coelenterazine for 3 h. They were sequentially treated with RPMI medium containing 0.01% (w/v) BSA, test peptide (1 μM), a standard and Triton X-100 (final 2.5%). Triton X-100 was used to lyse cells and confirm the expression of functionally active aequorin. The standard refers to one of the following positive controls: angiotensin II (1 μM), bradykinin (1 μM) and ATP (100 μM). A positive control that constantly exhibited higher signals than any other control was used as standard for a given organ, where bradykinin served as standard for pituitary and uterus, ATP for hypothalamus, liver and heart, and angiotensin II for adrenal gland. The mean relative luminescent units (RLU) elicited by the standards from 20 assays (values in parentheses indicate RLU ranges) for the pituitary, hypothalamus, liver, adrenal gland, uterus, and heart were 40,000 (23 000−51 500), 880 (200−3950), 160 (100−300), 2020 (120−9200), 11 600 (1700−32 000), and 820 (120−3000), respectively. Signals induced by test peptides were defined as positive in case RLUs were above 100 for the pituitary or 50 for the others, or above

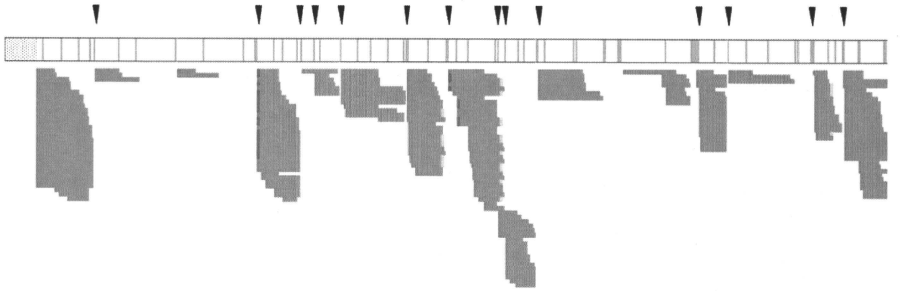

Figure 1. VGF processing deduced from identified peptides. Sequenced peptides are shown by gray boxes and detailed in Supplemental Table (Supporting Information). Closed arrowheads denote major cleavage sites across the top of the precursor, with basic residues (pale magenta boxes) and the signal sequence (a stippled box) indicated. Orange boxes, C-terminal amidation; red boxes, pyroglutamination.

5% of the RLUs induced by each standard in a given experiment. Peptides were dissolved in RPMI containing 0.01% (w/v) fatty acid-free BSA (Sigma) treated with activated charcoal. Data for test peptides were obtained from three or four independent experiments. A given peptide was considered positive on a tested tissue if positive signals were observed in at least two experiments. All the peptides were used at 1 μM throughout due to limited sensitivity inherent in this assay; endothelin-1, known as a potent vasoconstrictive peptide, did not produce a positive signal below 0.1 μM (data not shown).

Results and Discussion

The human thyroid cell line TT was stimulated with carbachol plus forskolin for 15 min to recover peptides secreted in the medium. The TT secretopeptidome was separated by gel filtration and subsequent cation exchange chromatography into 14 fractions for LC–MS/MS. Among the MS/MS-identified peptides, we studied peptides derived from VGF, a neurosecretory protein.[12,17] *Vgf*, expressed in various neurons and endocrine cells, encodes a 68-kDa protein of 617 amino acids in rodents and of 615 in human that bears several consensus motifs for processing enzymes PC1/3 and PC2 to yield peptides secreted via the regulated secretory pathway.[12] Studies of *Vgf*-deficient mice received much attention since they are lean, hypermetabolic, and resistant to various types of obesity.[18] These findings support the view that VGF is a precursor to multiple bioactive peptides. Major bioactive peptides derived from VGF are AQEE-30,[19] TLQP-62,[19] TLQP-21,[20] NERP-1 and NERP-2.[10] It is hence possible that additional bioactive peptides are embedded in this precursor sequence.

Consequently, we were able to identify 240 redundant peptides (155 distinct sequences) that arise from the human VGF sequence. These peptide sequences were aligned on the precursor sequence to construct a "peptide alignment map" (Figure 1 and Supplemental Figure 1, Supporting Information). Of note, this map is conceptually different from the peptide coverage map commonly used in proteomics studies. The peptide alignment map delineated 15 distinct clusters of the redundant peptides across the entire sequence. Consistent with the reported signal peptide,[12] the N-terminal region of 22 amino acids was not occupied by any peptide sequence (Figure 1). Each cluster consisted of peptides having N- or C-terminal trimming. The peptide ladders observed are not unique to VGF and common among different precursors of the regulatory secretion pathway, such as neuropeptide precursors and chromogranins identified in secretion media of endocrine cells, presumably caused by the action of exopeptidases.[14,21]

In 12 of 15 clusters, the longest peptide in each cluster was flanked by basic residue(s) at both ends (Figure 1 and Supplemental Figure 1, Supporting Information). Except for 232QARI MPD237, the boundaries that separate each cluster fit the consensus motifs for PC1/3 and PC2 ((R/K)Xn(R/K) where n = 0, 2, 4, or 6).[2] While not experimentally verified, the stretch of six basic residues 479KRKRKK484 may be a bona fide target of PC1/3, since PC1/3 actually cleaves the corresponding rat residues 483KRKRKK488.[22] Judging from the number of human peptides identified, APPG-40 (aa 23–62), QQET-30 (aa 177–206), MPDS-45 (aa 235–279), NERP-1 (aa 282–306, C-terminal amidation), NERP-2 (aa 310–347, C-terminal amidation), NAPP-19 (aa 485–503), and AQEE-30 (aa 586–615) were considered intact peptides released from TT cells. As noted earlier, NERP-1, NERP-2,[10] and AQEE-30[19] have been reported as bioactive. Although not illustrated by redundant identification (Supplemental Figure 1, Supporting Information), GGEE-45 (aa 373–417) also appeared to be an intact peptide.

The limited number of human VGF-derived peptides reported in cerebrospinal fluid peptitomics studies[23–25] does not suffice to elucidate an overall processing pattern of the precursor (Supplemental Figure 2, Supporting Information). In the present study, however, we were able to identify most, if not all, of potential processing sites of the precursor (Figures 1 and 2). While some of the clusters are represented by relatively few peptides (Figure 1), this might be caused by poor presentation of acidic peptides in positive ion mode, as exemplified by GGEE-45 with a calculated pI of 3.8. Otherwise, some regions may not have been appreciably converted to peptides in TT cells. For instance, the cleavage site 553RPRITLQ558 (corresponding human sequence 551RPRITLQ556) for the recently reported rat TLQP-21 as well as TLQP-62, an abundant C-terminal peptide in rat brain,[20] did not emerge in the TT secretopeptidome analysis. Since TT cells are of thyroid C-cell origin, the lack of identification might reflect the difference in cell type-specific precursor processing that involves multiple processing enzymes.[26] In two human pancreatic neuroendocrine cell lines we examined, we got evidence that 551RPRITLQ556 represented a major processing site (data not shown). To the

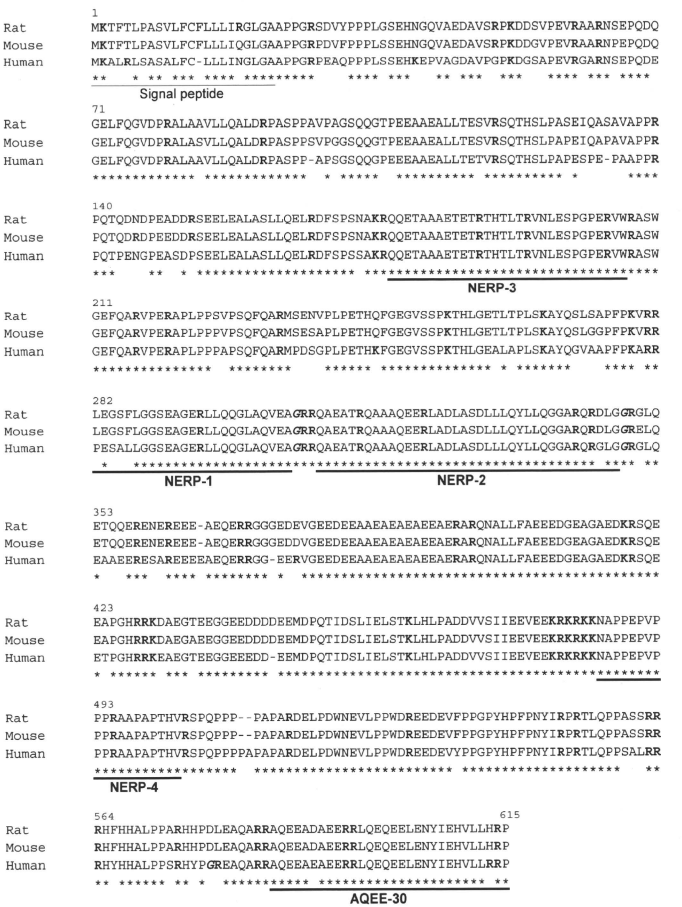

Figure 2. Alignment of rat (IPI00324864), mouse (IPI00378764), and human (IPI00069058) VGF sequences. Asterisks denote identical residues. Basic residues and amidation motifs are marked in bold and bold italic, respectively. The calcium assay was performed with bold underlined peptides. The residue numbering is for the human sequence.

best of our knowledge, this is the first study to demonstrate that accumulated peptide information contributes to elucidation of the overall processing of a precursor protein.

Bioactivity of a peptide cannot be inferred just from its sequence. It would be impossible to synthesize all of the peptides of various lengths revealed by LC–MS/MS. We therefore need to narrow down the number of candidate peptides for assessing bioactivity. In the present study, we took into consideration that peptides with definite biological activity are structurally conserved between species. Given the overall processing pattern (Figure 1), as well as interspecies homology between human and rodent VGF sequences (Figure 2), we selected QQET-30, hereafter designated NERP-3, and NAPP-19, designated NERP-4 (Figure 2). At the amino acid level, they are completely identical between human and rodents. APPG-40 and HYHH-19 (aa 565–583) were excluded since the location of internal basic residues is not conserved between rodent and human sequences (Figure 2). MPDS-45 was disregarded since rodent corresponding peptides were not so identical. HYHH-13 (aa 565–577, C-terminal amidation)[14] was also excluded because rodent VGF sequences do not harbor corresponding amidation sites. The stretch of acidic residues (seven aspartic and/or glutamic acids in human and eight in rodents) led us to disregard human EAEG-48 (aa 431–478. calculated p*I* 3.5). Also, the presence of multiple proline residues in SPQP-49 (aa

Table 1. Calcium Mobilization Induced by Test Peptides in Tissues from Apoaequorin Transgenic Mice[a]

	pituitary	hypothalamus	liver	adrenal gland	uterus	heart
NERP-3	+ (2/3)	+ (2/3)	− (0/3)	− (0/3)	− (0/3)	− (0/3)
NERP-4	+ (3/4)	+ (2/3)	− (0/3)	− (1/4)	− (0/3)	− (0/3)
AQEE-30	+ (2/4)	+ (2/3)	− (0/3)	− (1/4)	− (0/3)	− (0/3)
NERP-1	+ (3/3)	+ (2/3)	− (0/3)	ND	ND	ND
NERP-1-Gly	− (0/3)	− (0/3)	− (0/3)	ND	ND	ND
NERP-2	+ (3/3)	+ (2/3)	− (0/3)	ND	ND	ND
NERP-2-Gly	− (0/3)	− (0/3)	− (0/3)	ND	ND	ND

[a] Peptides were tested at a final concentration of 1 μM throughout. Data were summarized from at least three separate experiments. The peptide was considered active on the indicated tissue if positive signals were observed in at least two experiments. In parentheses, (X/Y) indicates the occurrence of positive signals (X) in total experiments (Y). ND, not determined.

505−553) was a reason for not including this peptide in subsequent assays.

Screening methods for bioactive peptides should be as comprehensive as possible. Given the presence of numerous cell types in an organism, a cell-based assay using a limited number of permanent cell lines or primary cultured cells is not practical. Since calcium is the most common second messenger, we used transgenic mice systemically expressing apoaequorin[11] to develop a tissue-based calcium assay. A candidate peptide is tested for its ability to raise intracellular calcium levels on selected tissues from the mice in a standardized analytical platform. Namely, the evoked calcium transient serves as a marker to report that the peptide is active on a tested tissue. The assay system was validated by bradykinin (pituitary) and ATP (hypothalamus, liver, and heart) and angiotensin II (adrenal gland) in advance. After an induced calcium transient returned to basal levels, expression of functional aequorin in the tested tissues was confirmed by lysing cells with Triton X-100. This treatment liberated intracellular apoaequorin to allow binding to extracellular calcium in incubation medium. At first, the utility of this assay system was assessed with the recently reported bioactive peptides NERP-1 and NERP-2[10] on pieces excised from the pituitary, hypothalamus, and liver. Consistent with their central actions reported in recent studies,[10] they elicited positive responses in the pituitary and hypothalamus (Figure 3 and Table 1). The inability of glycine-extended NERP-1 and NERP-2 to evoke the calcium response was also consistent with the previous report that NERPs' function is dependent on C-terminal amidation.[10] In this assay, the liver was considered a negative control since in most cases it does not respond to known bioactive peptides (data not shown).

NERP-3 and NERP-4, in addition to AQEE-30, were tested on the tissues including pituitary, hypothalamus, liver, adrenal gland, uterus, and heart. Aside from the liver, they are established targets for known neuropeptides and peptide hormones, including previously reported VGF-derived neuropeptides.[10,20] Positive signals were observed in the pituitary and hypothalamus in response to NERP-3 and NERP-4 (Figure 3 and Table 1). The observed calcium transient in the hypothalamus triggered by AQEE-30 may support a previous view that the peptide is a neuropeptide whose activity was first reported in isolated hypothalamic tissue cultures.[19] Overall, we identified two novel VGF-derived peptides that are functional toward the pituitary and hypothalamus.

As for human/mouse/rat NERP-3 and mouse/rat AQEE-30, we were able to prepare antibodies that specifically recognize

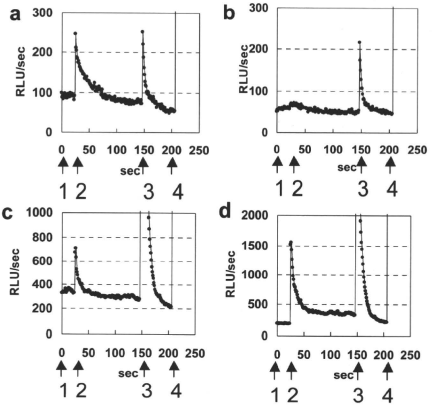

Figure 3. Typical traces of the relative luminescence units (RLU) evoked in hypothalamic tissues from apoaequorin transgenic mice. (a) NERP-1, (b) NERP-1-Gly, (c) NERP-3, and (d) AQEE-30. Peptides were tested at a final concentration of 1 μM. Medium (1), peptide (2), ATP (3), and Triton X-100 (4) were sequentially administered where indicated by arrows.

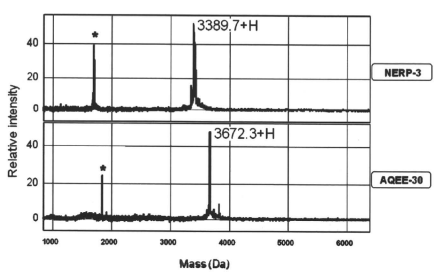

Figure 4. Mass characterization of peptides recognized by NERP-3 and AQEE-30 antibodies. Brain extract was immunoprecipitated with each antibody and analyzed on a surface-enhanced laser desorption ionization mass spectrometer. Asterisks indicate doubly charged ions.

the C-terminus of respective peptide as described in Materials and Methods. Peptides immunoprecipitated from whole rat brain extract were analyzed on a surface-enhanced laser desorption ionization mass spectrometer. Major peaks of the immunoprecipitate coincided with the calculated mass of 3389 Da (NERP-3) and 3672 Da (mouse/rat AQEE-30) (Figure 4), indicating that NERP-3 and AQEE-30 are actual major processing products also in rat brain. Although antibody was not prepared, NERP-4 may be a major peptide also in rodents as deduced by the multiple identifications in the human peptidomic data shown in Figure 1. Overall, this assay resulted in the identification of two VGF-derived peptides, designated NERP-3 and NERP-4, which are active on the pituitary and hypothalamus.

Conclusions

We described an approach to discover bioactive peptides and their target tissues. This approach can be extended to different

cell culture models. Identification of target organs or tissues will help to characterize responding cells and receptors.

Acknowledgment. We thank Emi Mishiro-Sato, Masako Matsubara (National Cerebral and Cardiovascular Center) and Miho Inoue, Machi Kusunoki, Teruyoshi Imada and Toyoko Kashiwagi (Kyowa Hakko Kirin) for expert technical assistance. This work was supported in part by the Program for Promotion of Fundamental Studies in Health Sciences of the National Institute of Biomedical Innovation, and by Grants-in-Aid for Scientific Research from the Japanese Society for the Promotion of Science, Japan. We also thank Junko Kimata, Makoto Takahata and Morihiko Yoshida (Thermo Fisher Scientific, Japan) for LTQ-Orbitrap operation.

Supporting Information Available: Supplemental Table, peptides identified by LC–MS/MS; Supplemental Figure 1, detailed presentation of Figure 1; Supplemental Figure 2, peptides reported in previous cerebrospinal peptidomics studies; Supplemental Figure 3, MS/MS spectra of peptides with modified residues listed in Supplemental Table. This material is available free of charge via the Internet at http://pubs.acs.org.

References

(1) Zhou, A.; Webb, G.; Zhu, X.; Steiner, D. F. Proteolytic processing in the secretory pathway. *J. Biol. Chem.* **1999**, *274*, 20745–8.
(2) Fricker, L. D. Neuropeptide-processing enzymes: applications for drug discovery. *AAPS J.* **2005**, *7*, E449–455.
(3) Eipper, B. A.; Stoffers, D. A.; Mains, R. E. The biosynthesis of neuropeptides: peptide alpha-amidation. *Annu. Rev. Neurosci.* **1992**, *15*, 57–85.
(4) Clynen, E.; Baggerman, G.; Veelaert, D.; Cerstiaens, A.; Van der Horst, D.; Harthoom, L.; Derua, R.; Waelkens, E.; De Loof, A.; Schoofs, L. Peptidomics of the pars intercerebralis-corpus cardiacum complex of the migratory locust, Locusta migratoria. *Eur. J. Biochem.* **2001**, *268*, 1929–39.
(5) Schrader, M.; Schultz-Knappe, P. Peptidomics technologies for human body fluids. *Trends Biotechnol.* **2001**, *10*, S55–60.
(6) Svensson, M.; Sköld, K.; Svenningsson, P.; Andren, P. E. Peptidomics-based discovery of novel neuropeptides. *J. Proteome Res.* **2003**, *2*, 213–9.
(7) Che, F. Y.; Lim, J.; Pan, H.; Biswas, R.; Fricker, L. D. Quantitative neuropeptidomics of microwave-irradiated mouse brain and pituitary. *Mol. Cell. Proteomics* **2005**, *4*, 1391–1405.
(8) Dowell, J. A.; Heyden, W. V.; Li, L. Rat neuropeptidomics by LC-MS/MS and MALDI-FTMS: enhanced dissection and extraction techniques coupled with 2D RP-RP HPLC. *J. Proteome Res.* **2006**, *5*, 3368–75.
(9) Bora, A.; Annangudi, S. P.; Millet, L. J.; Rubakhin, S. S.; Forbes, A. J.; Kelleher, N. L.; Gillette, M. U.; Sweedler, J. V. Neuropeptidomics of the rat supraoptic nucleus. *J. Proteome Res.* **2008**, *7*, 4992–5003.
(10) Yamaguchi, H.; Sasaki, K.; Satomi, Y.; Shimbara, T.; Kageyama, H.; Mondal, M. S.; Toshinai, K.; Date, Y.; Gonzalez, L. J.; Shioda, S.; Takao, T.; Nakazato, M.; Minamino, N. Peptidomic identification and biological characterization of neuroendocrine regulatory peptide-1 and -2. *J. Biol. Chem.* **2007**, *282*, 26354–60.
(11) Yamano, K.; Mori, K.; Nakano, R.; Kusunoki, M.; Inoue, M.; Satoh, M. Identification of the functional expression of adenosine A3 receptor in pancreas using transgenic mice expressing jellyfish apoaequorin. *Transgenic Res.* **2007**, *16*, 429–35.
(12) Levi, A.; Ferri, G. L.; Watson, E.; Possenti, R.; Salton, S. R. Processing, distribution, and function of VGF, a neuronal and endocrine peptide precursor. *Cell Mol. Neurobiol.* **2004**, *24*, 517–33.
(13) Gkonos, P. J.; Born, W.; Jones, B. N.; Petermann, J. B.; Keutmann, H. T.; Bimbaum, R. S.; Fischer, J. A.; Roos, B. A. Biosynthesis of calcitonin gene-related peptide and calcitonin by a human medullary thyroid carcinoma cell line. *J. Biol. Chem.* **1986**, *261*, 14386–91.
(14) Sasaki, K.; Satomi, Y.; Takao, T.; Minamino, N. Snapshot peptidomics of the regulated secretory pathway. *Mol. Cell. Proteomics* **2009**, *8*, 1638–47.
(15) Mishiro-Sato, E.; Sasaki, K.; Matsuo, Y.; Kageyama, H.; Yamaguchi, H.; Date, Y.; Matsubara, M.; Ishizu, T.; Yoshizawa-Kumagaye, K.; Satomi, Y.; Takao, T.; Shioda, S.; Nakazato, M.; Minamino, N. Distribution of neuroendocrine regulatory peptide-1 and−2, and proteolytic processing of their precursor VGF protein in the rat. *J. Neurochem.* **2010**, *114*, 1097–106.
(16) Sasaki, K.; Sato, K.; Akiyama, Y.; Yanagihara, K.; Oka, M.; Yamaguchi, K. Peptidomics-based approach reveals the secretion of the 29-residue COOH-terminal fragment of the putative tumor suppressor protein DMBT1 from pancreatic adenocarcinoma cell lines. *Cancer Res.* **2002**, *62*, 4894–8.
(17) Levi, A.; Eldridge, J. D.; Paterson, B. M. Molecular cloning of a gene sequence regulated by nerve growth factor. *Science* **1985**, *229*, 393–5.
(18) Hahm, S.; Mizuno, T. M.; Wu, T. J.; Wisor, J. P.; Priest, C. A.; Kozak, C. A.; Boozer, C. N.; Peng, B.; McEvoy, R. C.; Good, P.; Kelley, K. A.; Takahashi, J. S.; Pintar, J. E.; Roberts, J. L.; Mobbs, C. V.; Salton, S. R. Targeted deletion of the Vgf gene indicates that the encoded secretory peptide precursor plays a novel role in the regulation of energy balance. *Neuron* **1999**, *23*, 537–48.
(19) Alder, J.; Thakker-Varia, S.; Bangasser, D. A.; Kuroiwa, M.; Plummer, M. R.; Shors, T. J.; Black, I. B. Brain-derived neurotrophic factor-induced gene expression reveals novel actions of VGF in hippocampal synaptic plasticity. *J. Neurosci.* **2003**, *23*, 10800–8.
(20) Bartolomucci, A.; Possenti, R.; Levi, A.; Pavone, F.; Moles, A. The role of the vgf gene and VGF-derived peptides in nutrition and metabolism. *Genes Nutr.* **2007**, *2*, 169–80.
(21) Nikoulina, S. E.; Andon, N. L.; McCowen, K. M.; Hendricks, M. D.; Lowe, C.; Taylor, S. W. A primary colonic crypt model enriched in enteroendocrine cells facilitates a peptidomic survey of regulated hormone secretion. *Mol. Cell. Proteomics* **2010**, *9*, 728–41.
(22) Trani, E.; Giorgi, A.; Canu, N.; Amadoro, G.; Rinaldi, A. M.; Halban, P. A.; Ferri, G. L.; Possenti, R.; Schinina, M. E.; Levi, A. Isolation and characterization of VGF peptides in rat brain. Role of PC1/3 and PC2 in the maturation of VGF precursor. *J. Neurochem.* **2002**, *81*, 565–74.
(23) Selle, H.; Lamerz, J.; Buerger, K.; Dessauer, A.; Hager, K.; Hampel, H.; Karl, J.; Kellmann, M.; Lannfelt, L.; Louhija, J.; Riepe, M.; Rollinger, W.; Tumani, H.; Schrader, M.; Zucht, H.-D. Identification of novel biomarker candidates by differential peptidomics analysis of cerebrospinal fluid in Alzheimer's disease. *Comb. Chem. High Throughput Screen.* **2005**, *8*, 801–6.
(24) Huang, J. T.; Leweke, F. M.; Oxley, D.; Wang, L.; Harris, N.; Koethe, D.; Gerth, C. W.; Nolden, B. M.; Gross, S.; Schreiber, D.; Reed, B.; Bahn, S. Disease biomarkers in cerebrospinal fluid of patients with first-onset psychosis. *PLoS Med.* **2006**, *3*, e428.
(25) Zougman, A.; Pilch, B.; Podtelejnikov, A.; Kiehntopf, M.; Schnabel, C.; Kumar, C.; Mann, M. Integrated analysis of the cerebrospinal fluid peptidome and proteome. *J. Proteome Res.* **2008**, *7*, 386–99.
(26) Rehfeld, J. F.; Bundgaard, J. R.; Hannibal, J.; Zhu, X.; Norrbom, C.; Steiner, D. F.; Friis-Hansen, L. The cell-specific pattern of cholecystokinin peptides in endocrine cells versus neurons is governed by the expression of prohormone convertases 1/3, 2, and 5/6. *Endocrinology* **2008**, *149*, 1600–8.

PR1003455

Journal of Proteome Research | 3b2 | ver.9 | 12/2/011 | 4:57 | Msc: pr-2010-01114a | TEID: ram00 | BATID: 00000 | Pages: 10.8

Journal of proteome research

ARTICLE

pubs.acs.org/jpr

Peptidomics-Based Discovery of an Antimicrobial Peptide Derived from Insulin-Like Growth Factor-Binding Protein 5

Tsukasa Osaki, Kazuki Sasaki,* and Naoto Minamino*

Department of Molecular Pharmacology, National Cerebral and Cardiovascular Center Research Institute, Suita, Osaka 565-8565, Japan

Supporting Information

ABSTRACT: Antimicrobial peptides (AMPs) are effector molecules that are able to kill or inactivate microbial pathogens. However, most AMPs harbor multiple basic amino acids that hamper current proteomic identification. In our peptidomic survey of endogenous peptides, we identified a novel intramolecular disulfide-linked 22-residue amidated peptide. This peptide, designated AMP-IBP5 (antimicrobial peptide derived from insulin-like growth factor-binding protein 5), showed antimicrobial activity against six of the eight microorganisms tested at concentrations comparable to or lower than those for well-characterized AMPs cathelicidin and β-defensin-2. AMP-IBP5 is identical at the amino acid level between human, mouse, rat, pig, and cow. Natural occurrence of this peptide as the originally isolated form was demonstrated in the rat brain and intestine, using mass spectrometric characterization of major immunoreactivity. The peptide is flanked N-terminally by a single arginine and C-terminally by a common amidation signal, indicating that insulin-like growth factor-binding protein 5 (IGFBP-5) undergoes specific cleavage by a defined set of processing proteases. Furthermore, the intramolecular linkage C199-C210 reveals itself as a correct disulfide pairing in the precursor protein, the finding not inferred from closely related family members IGFBP-4 and -6. In principle, neither conventional proteomics nor bioinformatics would achieve the identification of this AMP. Our study exemplifies the impact of peptidomics to study naturally occurring peptides.

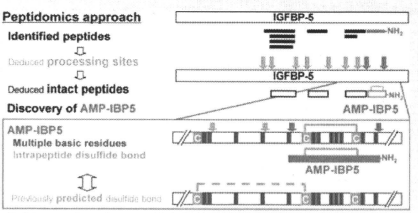

KEYWORDS: antimicrobial peptide, bioactive peptide, insulin-like growth factor-binding protein 5, mass spectrometry, peptidomics, proteolytic processing, secretopeptidome

INTRODUCTION

Bioactive peptides, such as peptide hormones and antimicrobial peptides (AMPs), have been identified through activity-guided biochemical purification that starts with a bulk of biological samples. Recently, technological advances in mass spectrometry (MS) enable us to identify naturally occurring peptides present in mixtures.[1−3] Nevertheless, we are faced with a daunting task of identifying bioactive peptides of a secretory nature owing to their relative low abundance. Once extracted from biological samples, secreted peptides are not discriminated from nonsecreted peptides or peptide fragments caused by degradation of cytosolic proteins. Since relatively abundant molecules are preferentially detected in MS schemes, we need to work on samples rich in secreted peptides for facilitating the discovery of bioactive peptides. We recently used tandem mass spectrometry (MS/MS) techniques to characterize a total pool of naturally occurring peptides that are released by exocytosis from cells in culture. This study, referred to as secretopeptidome analysis, allows us to identify peptides localized in secretory granules in a noninvasive as well as efficient manner.[4,5]

In the present study, we focused on secreted peptides with a highly basic nature. Some bioactive peptides, especially AMPs, harbor multiple basic amino acids. In fact, well-characterized mammalian AMPs β-defensin-2[6] and cathelicidin[7] both bear a net charge of +6 at pH 7.0. These peptides should be analyzed in their native forms, and therefore cannot be studied by current proteomics that needs an enzymatic digestion step for MS-based identification. We characterized highly basic fractions of the secretopeptidome from cultured human pancreatic neuroendocrine tumor cells and identified a previously unknown peptide that arises from insulin-like growth factor-binding protein 5 (IGFBP-5). With regard to antimicrobial activity and spectrum, this peptide is almost as potent as cathelicidin and even superior to β-defensin-2. The peptide was thus designated AMP-IBP5 (antimicrobial peptide derived from IGFBP-5). We provide evidence that AMP-IBP5 is generated through site-specific cleavages in the brain and small intestine. In addition, the identification of this intramolecular disulfide-linked peptide led us to conclude that IGFBP-5 protein possesses a disulfide pairing different from that previously predicted on the basis of analogy to IGFBP-4 and -6.[8] While bioinformatics is currently used for in silico prediction of bioactive peptides, this peptide could not be identified in a

Received: November 5, 2010

situation where we had relied on the previous incorrect disulfide pairing. Our data demonstrated that peptidomics is a promising tool to uncover previously uncharacterized peptides.

■ EXPERIMENTAL PROCEDURES

Peptide Preparation

Monolayer cultures of the human pancreatic neuroendocrine tumor cell line QGP-1[9] were rinsed three times with Hanks' medium (Invitrogen, Carlsbad, CA). Culture supernatant of the cells (ca. 3.2×10^7 cells) stimulated with 10 μM forskolin and 10 μM carbachol for 15 min was harvested. Peptides were extracted and gel-filtrated as previously described.[4] Cysteine residues of the gel-filtrated samples were converted to carbamidomethyl cysteines (CmC) using dithiothreitol and iodoacetamide, followed by desalting and lyophilization. Resultant products were dissolved in solvent A (10 mM ammonium formate, pH 3.8: acetonitrile (ACN) = 9:1 (v/v)) and applied to a TSK gel SP-2SW cation-exchange column (1.0 × 50 mm; TOSOH, Tokyo, Japan) equilibrated with solvent A, and eluted at a flow rate of 50 μL/min with a gradient of 0−100% solvent B (1 M ammonium formate, pH 3.8: ACN = 9:1 (v/v)) in 30 min and then maintained at 100% B for 20 min. Highly basic fractions eluted after 30 min and the preceding fractions eluted between 0 and 30 min were separately desalted and applied to a C18 PepMap column (0.075 × 150 mm; Dionex, Sunnyvale, CA) using an Ultimate liquid chromatography (LC) system (Dionex) equilibrated with solvent A (5% ACN, 0.1% trifluoroacetic acid (TFA)) at a flow rate of 300 nL/min. Peptides were eluted with four steps, 5% B (95% ACN, 0.1% TFA) in 5 min, a linear gradient of 5−60% B in 55 min, a linear gradient of 60−100% B in 5 min, and then 100% B in 20 min. Fractions were collected every 20 s from 10 min after sample injection and spotted onto a 384-well matrix-assisted laser desorption/ionization (MALDI) plate with an infusion of 1.75 mg/mL α-cyano-4-hydroxy cinnamic acid (Nacalai tesque, Kyoto, Japan) in 50% ACN, 0.1% TFA at a flow rate of 1.5 μL/min using a Probot microfraction collector (Dionex).

MS Analysis

Samples spotted on a MALDI plate were analyzed on a MALDI-TOF/TOF mass spectrometer (4800 Proteomics Analyzer, Applied Biosystems, Foster City, CA). Each spot was first analyzed in MS positive ion reflector mode in the mass range from 1000 to 5000 Da by accumulating signals of 1000 laser shots. The 15 most abundant parent ions with a signal-to-noise ratio >20 were selected for top-down MS/MS scans, excluding identical parent ions contained in adjacent spots from a given LC−MALDI run. MS/MS was conducted using medium collision energy in positive ion mode.

Data Analysis and Peptide Identification

Peak lists were generated by the "Launch Peaks to Mascot" function of 4000 Series Explorer software (ver. 3.5, Applied Biosystems) using the default parameters supplied by the manufacturer. Peak lists were searched against IPI Human (80128 entries on June 18, 2009) using Mascot (ver. 2.2), with no enzyme specification. Carbamidomethylation of cysteine was set as a fixed modification, and pyroglutamination and C-terminal amidation were simultaneously allowed as variable modifications. Peptide tolerance was set to 125 ppm and MS/MS tolerance was 0.4 Da. The significance threshold was the Mascot default setting of 5%. In Tables 1 and 2, peptides with a score above the identity threshold (corresponding to an expectation value below 0.05) were listed and considered identified.

Peptide Synthesis

Peptides derived from IGFBP-5 were synthesized on an Abacus peptide synthesizer (Sigma Genosys, Sigma Aldrich Japan, Hokkaido, Japan) using Fmoc (*N*-(9-fluorenyl) methoxycarbonyl) strategy, purified by reverse phase high performance liquid chromatography (HPLC), and verified for correct synthesis by MS and amino acid analysis. Purity of the peptides was confirmed on separate HPLC systems.

Heparin-Binding Assay

Synthetic peptides (1 nmol) were dissolved in 450 μL of phosphate-buffered saline (PBS, 10 mM phosphate buffer, pH 7.0 containing 0.15 M NaCl) and incubated with 50 μL of heparin-Sepharose CL-6B (GE Healthcare, Piscataway, NJ) at room temperature for 1 h. Supernatant was obtained by centrifugation at 800 × g for 3 min. Beads were washed three times with PBS (1 mL each). All the supernatants were combined as unbound fraction. After washing, bound peptides were eluted off the beads in 1 mL of 20 mM Tris-HCl, pH 8.0, containing 1.5 M NaCl (bound fractions). One-tenth volume of the bound and unbound fractions was each subjected to a reverse phase HPLC system. The linear gradient consisted of 10−60% ACN in 0.1% TFA for 40 min at a flow rate of 0.05 mL/min on a C18 reverse phase HPLC column (Vydac 218TP5115, 1.0 × 150 mm; Hesperia, CA). For a positive control of heparin-binding activity, cathelicidin (LL37; Bachem, Bubendorf, Switzerland) was used.[10]

Measurement of Antibacterial and Antifungal Activity

AlamarBlue (BioSource International, Camarillo, CA) was used to determine antimicrobial activity. As a consequence of bacterial growth, this oxidation−reduction indicator turns from blue to red in color. Antimicrobial activities of test peptides (up to 10 μM) or IGFBP-5 protein (1 μM; Ray Biotech, Norcross, GA) were assessed for the target microbes *Enterococcus hirae* (*E. hirae*), *Micrococcus luteus* (*M. luteus*), *Staphylococcus aureus* (*S. aureus*) 209P, *S. saprophyticus* KD, *Escherichia coli* (*E. coli*) B, *E. coli* K12, *E. coli* kp and *Pichia pastoris* (*P. pastoris*) GS115. The optimal growth temperature of *M. luteus*, *S. saprophyticus* KD and *P. pastoris* GS115 was 30 °C and that of the other microbes was 37 °C. After grown in 3% tryptosoy broth (Eiken Chemical, Tokyo, Japan) for 16 h with shaking at each optimal temperature, cells were washed twice with 10 mM phosphate buffer, pH 7.0, and diluted to 8×10^5 colony-forming units/ml in the same buffer. Twenty-five microliters of bacteria suspension was mixed with an equal volume of sample in the absence or presence of peptides, and incubated for 1 h. After incubation, 200 μL of 3% tryptosoy broth containing 10% alamarBlue was added to the reaction mixture and further incubated as follows: 4 h for *E. hirae*, *S. aureus* 209P and *E. coli* B; 6 h for *E. coli* K12 and *E. coli* kp; 7 h for *M. luteus*; 7.5 h for *S. saprophyticus* KD; and 20 h for *P. pastoris* GS115. Aliquots containing all assay reagents but microbes were used as blank. After incubation, the reactions were monitored by absorbance at 570 and 600 nm. Molar extinction coefficients of OD_{570} and OD_{600} in the oxidative condition are 80586 and 117216. Therefore, viability (%) was expressed using the following formula: viability (%) = $(117216 \times OD_{570} - 80586 \times OD_{600}$ in the presence of peptides$/117216 \times OD_{570} - 80586 \times OD_{600}$ in the absence of peptides$) \times 100$. The classical colony formation assay was also performed as described[11,12] using *S. aureus* 209P, *E. coli* K12 and *P. pastoris* GS115. For positive controls of

Table 1. Peptides Identified in Highly Basic Fractions[a]

precursor	IPI accession	m/z (obsd)	M_r (calc) (Da)	mass error (Da)	MASCOT score	expect.	N-term	peptide	C-term	net charge (pH 7.0)
CgA	00383975	1779.87	1778.93	−0.07	63	0.026	L	SFRARAYGFRGPGPQL	R	+3
CgB	00006601	2460.91	2460.12	−0.21	125	6.90×10^{-9}	M	AHGYGEESEEERGLEPGKGRHH	R	−3
CgB	00006601	1995.79	1994.94	−0.16	83	0.00018	R	FLGEGHHRVQENQMDKA	R	−1
CgB	00006601	1952.87	1952.03	−0.17	65	0.0044	R	GLEPGKGRHHRGRGGEPR	A	+3
CgB	00006601	2106.84	2105.98	−0.15	59	0.011	R	SETHAAGHSQEKTHSREKS	S	−1
CGRP	00027855	2390.12	2389.32	−0.21	98	9.70×10^{-6}	G	LLSRSGGVVKNNFVPTNVGSKAF-NH2	G	+4
CT	00000914	2435.85	2435.07	−0.23	69	0.0013	R	DMSSDLERDHRPHVSMPQNAN	C-term	−2
DSG2	00028931	1822.88	1822.03	−0.16	99	1.70×10^{-6}	R	NENKLLPKHPHLVRQ	K	+2
IGFBP5	00029236	2770.21	2769.44	−0.24	61	0.046	R	AVYLPNCDRKGFYKRKQCKPSR-NH2	G	+7
NUCB1	00893068	1580.70	1579.85	−0.16	72	0.0031	R	ELDFVSHHVRTKL	D	0
PC2	00643663	3111.38	3110.55	−0.18	73	0.0031	R	<QVAAEHGFGVRKLPFAEGLYHFYHNGLA	K	−1
PC2	00643663	2423.07	2422.24	−0.18	116	3.20×10^{-8}	A	ERPVFTNHFLVELHKGGEDKA	R	−1
PC2	00643663	1976.90	1975.99	−0.10	109	7.20×10^{-7}	R	KLPFAEGLYHFYHNGLA	K	0
PC2	00643663	1390.57	1389.71	−0.15	71	0.0037	R	SLHHKQQLERD	P	−1
PC2	00643663	1643.71	1642.87	−0.16	87	9.30×10^{-5}	R	SLHHKQQLERDPR	V	+1
SST	00000130	1157.44	1156.55	−0.11	70	0.0024	K	AGCKNFFWK	T	+2
SST	00000130	1258.48	1257.60	−0.12	67	0.0054	K	AGCKNFFWKT	F	+2
SST	00000130	1593.64	1592.74	−0.11	59	0.043	K	AGCKNFFWKTFTS	C	+2
SST	00000130	1753.62	1752.78	−0.17	77	7.10×10^{-5}	K	AGCKNFFWKT FTSC	C-term	+2
SST	00000130	1625.61	1624.72	−0.11	86	6.40×10^{-5}	G	CKNFFWKTFTSC	C-term	+2
SST	00000130	1334.54	1333.63	0.10	74	0.0016	A	GCKNFFWKTF	T	+2
SST	00000130	1682.63	1681.74	−0.12	91	1.90×10^{-5}	A	GCKNFFWKTFTSC	C-term	+2
VGF	00289501	3706.59	3705.83	−0.25	69	0.0071	R	AQEEAEAEERRLQEQEELENYIEHVLLRRP	C-term	−6
VGF	00289501	1786.80	1785.90	−0.11	70	0.0062	H	HALPPSRHYPGREAQA	R	+1
VGF	00289501	1724.74	1723.87	−0.13	70	0.0052	Y	HHALPPSRHYPGREA	Q	+1
VGF	00289501	1923.82	1922.96	−0.15	88	1.80×10^{-5}	Y	HHALPPSRHYPGREAQA	R	+1
VGF	00289501	1351.55	1350.67	−0.13	68	0.0065	R	HYHHALPPSRH	Y	+1
VGF	00289501	1953.80	1952.95	−0.16	53	0.05	R	HYHHALPPSRHYPGRE	A	+1
VGF	00289501	2024.81	2023.99	−0.18	89	1.10×10^{-5}	R	HYHHALPPSRHYPGREA	Q	+1
VGF	00289501	2152.91	2152.05	−0.15	88	1.60×10^{-5}	R	HYHHALPPSRHYPGREAQ	A	+1
VGF	00289501	2223.91	2223.08	−0.18	94	4.20×10^{-6}	R	HYH HALPPSRHYPGREAQA	R	+1
VGF	00289501	1610.68	1609.80	−0.13	69	0.0052	R	HYHHALPPSRHYP-NH2	G	+2
VGF	00289501	2380.01	2379.18	−0.18	54	0.043	R	RHYH HALPPSRHYPGREAQA	R	+2
VGF	00289501	1766.75	1765.90	−0.16	79	0.00065	R	RHYHHALPPSRHYP-NH2	G	+3
VGF	00289501	2564.15	2563.35	−0.21	121	9.50×10^{-9}	R	RLQEQEELENYIEHVLLRRP	C-term	−2
VGF	00289501	1594.76	1593.89	−0.14	66	0.014	R	TLQPPSALRRRHY	H	+3
VGF	00289501	2086.87	2086.02	−0.16	68	0.008	H	YHHALPPSRHYPGREAQA	R	0

[a] Peptides whose expectation values (Expect., column 7) were less than 0.05 are listed. M_r (calc) represents the theoretical monoisotopic molecular mass (Da) of the peptide sequence. MASCOT scores are indicated in column 6. The N-terminal (N-term) and C-terminal (C-term) flanking one amino acid (columns 8 and 10) are shown. Net charge (pH 7.0) was calculated as follows: D and E are −1, K and R are +1, and H is 0. N-terminal amino group is +1, and C-terminal carboxyl group is −1. <Q, pyroglutamic acid; -NH2, C-terminal amidation. CgA, chromogranin A; CgB, chromogranin B; CGRP, calcitonin gene-related peptide; CT, calcitonin; DSG2, desmoglein 2; IGFBP5, insulin-like growth factor-binding protein 5; NUCB1, nucleobindin 1; PC2, prohormone convertase 2; SST, somatostatin.

dx.doi.org/10.1021/pr101114q | J. Proteome Res. XXXX, XXX, 000–000

Table 2. IGFBP-5-Derived Peptides Identified by Mass Spectrometry[a]

m/z (obsd)	M_r (calc) (Da)	mass error (Da)	MASCOT score	identity threshold	expect.	N-term	peptide	C-term
3332.62	3331.54	0.07	134	54	5.50×10^{-10}	VKIER	DSREHEEPTTSEMAEETYSPKIFRPKH	RISEL
2974.46	2973.38	0.07	165	54	4.10×10^{-13}	ERDSR	EHEEPTTSEMAEETYSPKIFRPKHT	RISEL
2956.13	2955.37	−0.25	154	57	1.10×10^{-11}	ERDSR	<EHEEPTTSEMAEETYSPKIFRPKHT	RISEL
2873.41	2872.33	0.07	80	54	0.00013	ERDSR	EHEEPTTSEMAEETYSPKIFRPKH	TRISE
1812.88	1811.93	−0.05	143	54	7.80×10^{-11}	DRRKK	LTQSKFVGGAENTAHPR	IISAP
2080.34	2079.07	0.26	71	50	0.0005	GPCRR	HMEASLQELKASPRMVPR	AVYLP
1596.80	1595.81	−0.01	72	54	0.00097	GPCRR	HMEASLQELKASPR	MVPRA
2770.21	2769.44	−0.24	61	60	0.046	RMVPR	AVYLPNCDRKGFYKRKQCKPSR-NH2	GRKRG

[a] Peptides whose MASCOT scores (column 4) exceeded identity thresholds (column 5) are listed. Mr (calc) represents the theoretical monoisotopic molecular mass (Da) of the peptide sequence. Expectation values (Expect.) are indicated in column 6. The N-terminal (N-term) and C-terminal (C-term) flanking five amino acid sequences (columns 7 and 9) are shown. <E, pyroglutamic acid; -NH2, C-terminal amidation.

antimicrobial activity, cathelicidin and β-defensin-2 (Peptide Institute, Osaka, Japan) were used.

Statistical Analysis

Statistical analysis was performed using Student's *t* test, with a level of significance set at $p < 0.05$.

Preparation of Cell Culture Supernatant

The culture supernatant from QGP-1 was prepared as described above. Monolayer culture of the human lung neuroendocrine tumor cell line SHP-77[13] (Ca. 1.1×10^7 cells) was stimulated with 50 mM potassium chloride and 10 μM carbachol for 10 min and its culture supernatant was harvested. Peptides were extracted as previously described[4] and used for radioimmunoassay (RIA).

Tissue Collection from Sprague-Dawley Rats

All experimental procedures of tissue collection from rats and immunization of rabbits were approved by our institutional animal experiments and care committee. Brain, pituitary gland, lung, heart, stomach, small intestine, liver, pancreas, kidney and uterus were collected from three female Sprague-Dawley rats (11-week-old, 220−280 g) immediately after decapitation, and used for RIA.

Antibody Preparation

Synthetic AMP-IBP5 (AVYLPNCDRKGFYKRKQCKPSR-NH_2, intramolecularly disulfide-linked) was conjugated with bovine thyroglobulin (Sigma Aldrich, St. Louis, MO) by the action of water-soluble carbodiimide (Peptide Institute). Rabbits were immunized with each conjugate emulsified with an equal volume of Freund's complete adjuvant as reported.[14]

RIA

RIA was carried out as reported[15] using intramolecularly disulfide-linked ^{125}I-radiolabeled YAVYLPNCDRKGFYKRKQ-CKP SR-NH_2 and anti-AMP-IBP5 antibody (#569−5) at a dilution of 1:210 000. A fifty percent inhibitory concentration (IC_{50}) of ligand binding in the RIA was 20 fmol/tube. Specificity of the RIA was examined with C-terminally Gly-extended AMP-IBP5, carbamidomethylated (CAM)-AMP-IBP5, IGFBP-5 protein and seven known bioactive peptides, vasopressin, calcitonin, adrenomedullin, proadrenomedullin N-terminal 20-amino acid peptide (PAMP-20), neurokinin A, angiotensin II and leucine-enkephalin. The six bioactive peptides except PAMP-20 showed no cross-reactivity up to 100 000 fmol/tube, and IGFBP-5 protein had no cross-reactivity up to 10 000 fmol/tube. The IC_{50} values of C-terminally Gly-extended AMP-IBP5, CAM-AMP-IBP5, and PAMP-20 (arginine amide) were 20 000, 20, and 100 000 fmol/tube, respectively. These results indicate that the antiserum strictly recognizes the C-terminal region including amide structure but not the disulfide bond or the intact IGFBP-5 protein.

Immunological Detection of AMP-IBP5

Tissues were collected as described above, extracted and condensed with a Sep-Pak C18 cartridge as described previously.[16] An aliquot of cartridge eluate was examined by RIA to quantify immunoreactive (IR)-AMP-IBP5. Brain and small intestine extracts were loaded onto a gel filtration column (Sephadex G-50 fine, GE Healthcare; 1.8 × 135 cm) equilibrated with 1 M CH_3COOH at a flow rate of 7 mL/h, fractionated every 6 mL/tube, and assessed by RIA to evaluate an IR-AMP-IBP5 level in each fraction. Fractions containing most abundant IR-AMP-IBP5 were pooled, lyophilized, and separated on a reverse phase HPLC column (Symmetry300 C18 5 μ, 4.6 × 250 mm; Waters Co., Milford, MA) equilibrated with solvent A (10% ACN, 0.1% TFA) at a flow rate of 1 mL/min. Adsorbed samples were eluted with a linear gradient of 0−100% B (60% ACN, 0.1% TFA) in 60 min, fractionated every 1 mL/tube, and assessed by RIA.

For MS of immunoprecipitates, the fraction containing a highest level of IR-AMP-IBP5 in the reverse phase HPLC was lyophilized, dissolved in 40 μL of the antibody (#569-5) 10-fold diluted with PBS, and incubated overnight with 10 μL of Protein A-Sepharose CL-4B (GE Healthcare) at 4 °C. Immunocomplexes were washed three times with PBS and twice with distilled water (1 mL each), followed by elution in 20 μL of 1% TFA and desalting using u-C18 Zip Tips (Millipore, Billerica, MA). Recovered AMP-IBP5-IR materials were spotted on target plates with α-cyano-4-hydroxy cinnamic acid matrix and then analyzed in MS positive ion reflector mode in the mass range from 1000 to 5000 Da on a 4800 Proteomics Analyzer.

SDS-PAGE and Immunoblotting

Tissues were collected as described above and extracted with 10 volumes (w/v) of SDS-PAGE loading buffer, followed by separation on a 15% SDS-PAGE gel and transfer to a PVDF membrane (GE Healthcare) as reported.[17] Membranes were probed with the first antibody and then probed with horseradish peroxidase-conjugated goat antirabbit IgG (1:5000; Cell Signaling Technology, Beverly, MA). First antibodies were used as follows: a rabbit polyclonal antibody (H-100) raised against human IGFBP-5[81-180] (1:1000; Santa Cruz Biotechnology, Santa Cruz, CA) for detecting intact IGFBP-5; and a rabbit monoclonal antibody (14C10) raised against human/rat glyceraldehyde 3-phosphate dehydrogenase (GAPDH) (1:5000; Cell

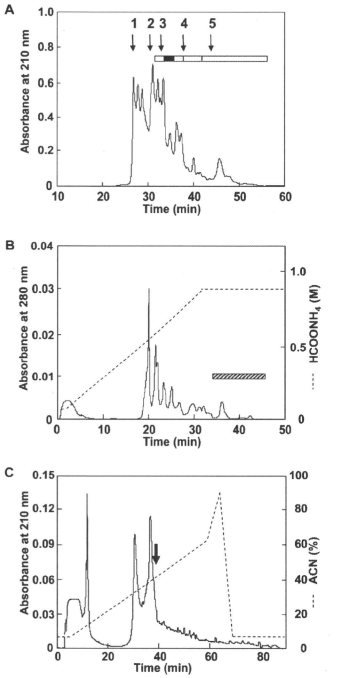

Figure 1. Preparation of highly basic peptides for peptidomic analysis. (A) Gel filtration profile of culture supernatant extracts from QGP-1 cells. Peptide-containing fractions were indicated by five boxes; the closed box indicated the fraction in which AMP-IBP5 originated. Molecular weight makers: 1, bovine serum albumin (66.5 kDa); 2, ribonuclease A (13.5 kDa); 3, neuropeptide Y (4.3 kDa); 4, neurotensin (1.7 kDa) and 5, Leu-enkephalin (0.6 kDa). (B) Cation-exchange HPLC of the AMP-IBP5-containing fraction obtained by the preceding gel filtration. Fractions eluted between 35 and 46 min (hatched box) were pooled for LC-MALDI-MS. (C) Subsequent nanoLC separation of the fraction denoted by the hatched box in (B). AMP-IBP5 was identified at the arrowed microfraction.

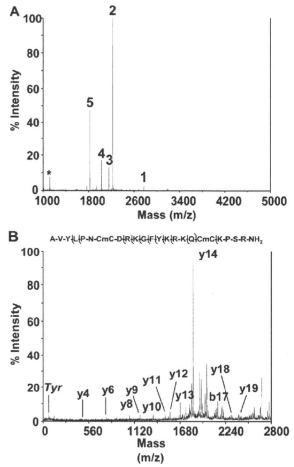

Figure 2. MS identification of AMP-IBP5. (A) MS spectrum from the microfraction indicated by the arrow in Figure 1C. 1, IGFBP-5[193-214]-NH_2 (AMP-IBP5) AVYLPNCDRKGFYKRKQCKPSR-NH_2; 2, VGF[543-561] HYHHALPPSRHYPGREAQA; 3, VGF[543−560]; 4, VGF[543-559]; 5, Desmoglein 2[10-24] NENKLLPKHPHLVRQ; *, double charged ions of 2. (B) MS/MS identification of AMP-IBP5. The peptide was identified with one b-ion and eleven y-ions. *Tyr* denotes the immonium ion of Tyr.

Signaling Technology). Membranes were visualized using an ECL-plus kit, according to the protocol provided by the manufacturer (GE Healthcare), and images were recorded with a LAS-1000 plus imager (Fujifilm, Tokyo, Japan) for 1−10 min. Digital images were quantitated using Image J software (National Institutes of Health, Bethesda, MD).

■ RESULTS

Peptidomic Identification of IGFBP-5-Derived Peptides

We recovered the culture supernatant from QGP-1 cells that received an exocytotic stimulus of 10 μM forskolin plus 10 μM carbachol for 15 min. Substances extracted from the supernatant were separated by gel filtration HPLC to obtain peptides distributed over five fractions (Figure 1A, open and closed boxes). These five fractions were each subjected to reductive alkylation and further separated by cation-exchange HPLC (Figure 1B). To obtain a highly basic fraction, peptides eluted over the ammonium formate concentration of 0.9 M (pH 3.8) (Figure 1B, hatched box) were pooled for subsequent LC-MALDI-MS analysis. Table 1 summarizes a list of MS/MS-identified peptides in these basic fractions obtained by the cation-exchange separations. We identified 37 peptides, of which 35 peptides arose from precursor proteins reported to be enriched in secretory granules,[4,18] including VGF, somatostatin, prohormone convertase 2 (PC2), chromogranin A, chromogranin B, calcitonin gene-related peptide, calcitonin and nucleobindin 1. Among the identified peptides, AVYLPN(CmC)DRKGFY-KRKQ(CmC)KPSR-NH_2 was derived from IGFBP-5 and found to be unique with a net charge of +7 even at pH 7.0 (Table 1). The closed box (Figure 1A), the hatched box (Figure 1B) and the arrow (Figure 1C) indicate the fractions in which this peptide originated. MS profiling of the microfraction indicated by the arrow in Figure 1C showed the signal of this peptide (Figure 2A, peak 1), whose sequence was identified by MS/MS (Figure 2B and Supplementary data).

IGFBP-5 is a secreted protein, but its proteolytic processing and concomitant generation of functional peptides remained unknown. To search for different IGFBP-5-derived peptides, we analyzed other fractions of the secretopeptidome by LC-MALDI-MS/MS. As shown in Table 2 and Figure 3, we identified a total of eight distinct peptides derived from IGFBP-5. This result

dx.doi.org/10.1021/pr101114a |J. Proteome Res. XXXX, XXX, 000-000

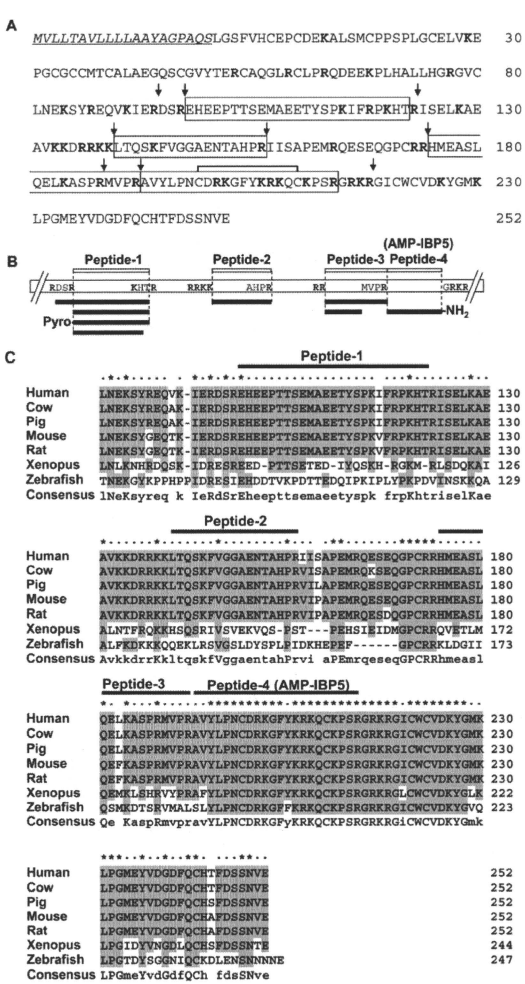

Figure 3. Peptides processed from IGFBP-5 and sequence alignment of IGFBP-5 between various vertebrates. (A) Amino acid sequence of human IGFBP-5. Signal sequence is indicated in italic and underlined. Basic amino acids, K and R, are denoted by bold letters. Four distinct regions from which peptides are processed out are boxed as follows: Peptide-1, IGFBP-5[98-122]; Peptide-2, IGFBP-5[140-156]; Peptide-3, IGFBP-5[175-192]; Peptide-4 (AMP-IBP5), IGFBP-5[193-214]-NH_2. The disulfide-bond (C199-C210) determined in this study is shown by the bold line. Processing sites predicted by identified peptides (Figure 3B) are indicated by arrows. (B) Identified peptides derived from IGFBP-5. Peptides listed in Table 2 are denoted by closed boxes. Above the entire precursor, open boxes indicate synthesized peptides. Basic amino acids in the processing sites are denoted by bold letters. Pyro- and -NH_2 mean N-terminal pyroglutamination and C-terminal amidation, respectively. (C) Sequence alignment of the central and C-terminal domains of various vertebrate IGFBP-5s. Residues conserved in more than four species are shaded. Asterisks indicate the completely conserved residues and dots indicate residues conserved in more than four vertebrates. Consensus amino acid residues conserved completely and in more than four species are indicated by upper and lower cases, respectively. Accession numbers of IGFBP-5: human, NP_000590.1; cow, NP_001098797.1; pig, NP_999264.1; mouse, NP_034648.2; rat, NP_036949.1; *Xenopus*, NP_001083938.1; and zebrafish, NP_991289.1. Residue numbering for zebrafish is based on the signal sequence prediction by SignalIP 3.0 Server (http://www.cbs.dtu.dk/services/SignalP/).

dx.doi.org/10.1021/pr101114a |*J. Proteome Res.* XXXX, XXX, 000–000

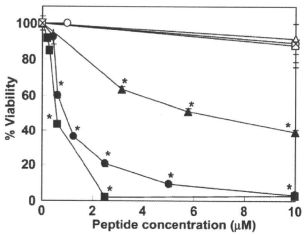

Figure 4. Antimicrobial activity of AMP-IBP5 against *Escherichia coli* K12. Increasing amounts of AMP-IBP5 (●, 0.3 to 10 μM) were mixed with *E. coli* K12 and incubated for 1 h at 37 °C. Antimicrobial activity was assayed as described under "Experimental procedures." Other IGFBP-5-derived peptides, Peptide-1 (Δ, 10 μM), Peptide-2 (□, 10 μM) and Peptide-3 (×, 10 μM), and IGFBP-5 protein (○, 1 μM) were also mixed with *E. coli* K12 and incubated as described above. As a positive control, increasing amounts of β-defensin-2 (▲, 3.2 to 10 μM) and cathelicidin (■, 0.2 to 10 μM) were used.

suggests that IGFBP-5 undergoes proteolytic processing to produce some functional peptides.

In neurons and endocrine cells, many peptides released by exocytosis are processed by PC1/3 or PC2.[19,20] Identification of the PC2-derived peptides, corresponding to the propeptide region, suggests the expression of functional PC2 in the cell line examined (Table 1). We deduced processing sites of the eight peptides from IGFBP-5 while considering their sequence information (Figure 3A) as well as substrate specificity of the PCs.[19,20] **RDSR**, **KHTR**, **RRKK**, **RR**, and **GRKR** shown in Figure 3B are typical processing sites for the PCs. We surmised that peptides are processed out from four distinct regions of this precursor protein, tentatively designated Peptide-1 to Peptide-4 in the order from N-terminus, and synthesized these peptides (Figure 3A). At the amino acid sequence level, Peptide-4 is completely identical among mammals and highly homologous between mammals and nonmammals (*Xenopus* and zebrafish) (Figure 3C). Collectively, this high sequence conservation of Peptide-4 suggests that this peptide contains a biologically active unit. In fact, a consensus sequence for heparin binding XBBBXXBX (where X is a hydrophobic or uncharged residue and B is a basic residue)[10] is present in Peptide-4 (13Y**KRK**Q**CK**P20). In contrast with Peptide-4, Peptide-1 to Peptide-3 did not show marked homology between mammals and nonmammals (Figure 3C).

Antimicrobial Activity of IGFBP-5-Derived Peptides

Cationic peptides that contain heparin-binding consensus sequences have been shown to exert antimicrobial activity.[10] As described above, Peptide-4 contains the consensus sequence and, in fact, Peptide-4 as well as cathelicidin bound to heparin, while Peptid-1 to Peptide-3 did not (Supplementary Figure 1C, F, Supporting Information). These results, in addition to the extremely basic nature of Peptide-4 with a net charge of +7 at pH 7.0 (Table 1), suggested that Peptide-4 exerts antimicrobial activity which we examined using a metabolic indicator alamarBlue™. Peptide-4 showed a significant antimicrobial activity against *E. coli* K12 at more than 0.6 μM, while Peptide-1 to Peptide-3 were not effective against *E. coli* K12 even at 10 μM (Figure 4). The IC_{50} value of Peptide-4 was almost equal to or lower than those for well-characterized AMPs cathelicidin and β-defensin-2. These values of the AMPs consistent with those reported in previous studies.[21,22] Notably, the parent protein IGFBP-5 was ineffective even at 1 μM (Figure 4). Given these data, we renamed Peptide-4 as AMP-IBP5 (antimicrobial peptide derived from IGFBP-5).

To determine the antimicrobial spectrum of AMP-IBP5, we tested four-types of Gram-positive bacteria (*E. hirae*, *M. luteus*, *S. aureus* 209P and *S. saprophyticus* KD), two other Gram-negative bacteria (*E. coli* B and *E. coli* kp) and one fungus (*P. pastoris* GS115) (Table 3). AMP-IBP5 showed a broad and strong spectrum of antimicrobial activity except for two types of Gram-positive bacteria (*E. hirae* and *S. saprophyticus* KD). Of note, AMP-IBP5 was active against *M. luteus* and *P. pastoris* GS115, even greater than cathelicidin and β-defensin-2. AMP-IBP5 showed the activity against *S. aureus* 209P, *E. coli* B and *E. coli* kp, which were weaker than cathelicidin and greater than β-defensin-2. These results indicate that AMP-IBP5 shows an antimicrobial spectrum and activity almost equal to cathelicidin and greater than β-defensin-2.

We next assessed CAM-AMP-IBP5 to investigate the role of a disulfide linkage. Cysteine-rich AMPs such as defensins are structurally stabilized by intramolecular disulfide linkages that are essential for their function.[23] In fact, CAM-β-defensin-2 did not show antimicrobial activity against various bacteria except for *M. luteus* (Table 3). As for CAM-AMP-IBP5, antimicrobial activity was abrogated for *S. aureus* 209P and *E. coli* kp, to which it was still active, though more than five-fold weaker than the intact form. On the other hand, this peptide retained the activity against *M. luteus*, *E. coli* B and *P. pastoris* GS115 comparable to the intact peptide, while the modified peptide showed about 2-fold weaker activity against *E. coli* K12 than the intact peptide. These results indicate that the disruption of disulfide linkages in AMP-IBP5 is less effective in reducing antimicrobial activity than that in β-defensin-2 presumably because the former contains only one disulfide linkage while the latter contains three disulfide linkages.

Some AMPs have the C-terminal amide group that plays a significant role in their antimicrobial properties.[24,25] We measured antimicrobial activity of C-terminally Gly-extended AMP-IBP5 to evaluate the contribution of the C-terminal amide group. It showed no activity against *S. aureus* 209P, *E. coli* B and *E. coli* kp as well as *E. hirae* and *S. saprophyticus* KD. On the other hand, this peptide retained the activity against *M. luteus* and *P. pastoris* GS115 comparable to the intact peptide, while the modified peptide was about 10-fold weaker against *E. coli* K12 than the intact peptide. These results indicate that the C-terminal amide group of AMP-IBP5 is important for its activity.

To examine whether AMP-IBP5 is bactericidal or just bacteriostatic, we performed a classical colony formation assay. It has been established that the bactericidal peptide concentration revealed by classical colony formation assays and the alamarBlue™ assay shows a good agreement.[26−28] As expected, this peptide showed strong antimicrobial activity with IC_{50} of 1.6, 1.1, and 0.4 μM against *S. aureus* 209P, *E. coli* K12 and *P. pastoris* GS115, respectively (Table 4). These IC_{50} values were also almost equal to or lower than that for cathelicidin and β-defensin-2 as in the case of the alamarBlue assay. These results indicate that AMP-IBP5 is bactericidal against these bacteria.

Immunological and Mass Spectrometric Characterization of IR-AMP-IBP5

We developed a RIA system specific to the C-terminal region including amide structure (see "Experimental Procedures") to

dx.doi.org/10.1021/pr101114a |*J. Proteome Res.* XXXX, XXX, 000–000

Table 3. Antimicrobial Activity of AMP-IBP5, β-Defensin-2, and Cathelicidin (alamarBlue Assay)

	$IC_{50}(\mu M)^a$					
	AMP-IBP5			β-defensin-2		cathelicidin
	intact[b]	CAM[b]	C-Gly[b]	intact[b]	CAM[b]	intact[b]
Gram-positive bacteria						
Enterococcus hirae	>10	>10	>10	2.4	>10	0.3
Micrococcus luteus	0.5	0.7	0.8	0.7	3.9	1.3
Staphylococcus aureus 209 P	0.8	>10	>10	8.6	>10	0.3
Staphylococcus saprophyticus KD	>10	>10	>10	>10	>10	0.6
Gram-negative bacteria						
Escherichia coli B	8.8	7.6	>10	>10	>10	0.5
Escherichia coli K12	0.9	2.2	9.3	6.3	>10	0.6
Escherichia coli kp	4.2	>10	>10	7.4	>10	1.7
Fungi						
Pichia pastoris GS115	1.3	1.5	1.6	2.6	>10	3.1

[a] Fifty percent growth inhibitory concentration. [b] Intact, intact peptide; CAM, carbamidomethylated peptide; C-Gly, C-terminally Gly-extended peptide.

Table 4. Antimicrobial Activity of AMP-IBP5, β-Defensin-2, and Cathelicidin (Colony Formation Assay)

	IC_{50} (μM)		
	AMP-IBP5	β-defensin-2	cathelicidin
Gram-positive bacteria			
Staphylococcus aureus 209 P	1.6	3.9	0.03
Gram-negative bacteria			
Escherichia coli K12	1.1	>10	0.4
Fungi			
Pichia pastoris GS115	0.4	1.0	1.2

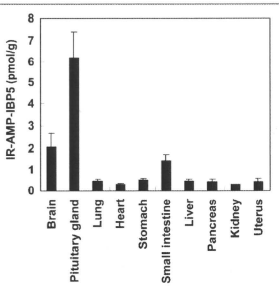

Figure 5. Determination of IR-AMP-IBP5 levels in rat tissues by RIA. Data are the mean ± SD (n = 3). The detection limit for quantitative measurement is 0.6 pmol/g wet tissues.

determine IR-AMP-IBP5 levels released from QGP-1 cells with or without stimulation by carbachol plus forskolin (10 μM each) for 15 min. The exocytosis stimulus caused a 500-fold increase in IR-AMP-IBP5 levels; the amounts secreted per 10^7 cells before and after 15-min stimulation were 4.9 fmol and 2.6 pmol, respectively. We also determined IR-AMP-IBP5 levels released from SHP-77 cells with or without stimulation by carbachol (10 μM) plus potassium chloride (50 mM) for 10 min. The exocytosis stimulus caused a 5-fold increase in IR-AMP-IBP5 levels; the amounts secreted per 10^7 cells before and after 10-min stimulation were 140 fmol and 650 fmol, respectively.

We determined AMP-IBP5 levels in rat tissues using the same RIA system. IR-AMP-IBP5 in the brain, pituitary gland and small intestine was 2.1, 6.2, and 1.5 pmol/g wet tissues, respectively. In the lung, heart, stomach, liver, pancreas, kidney and uterus, it was below the detection limit for quantitative measurement (0.6 pmol/g wet tissue) (Figure 5). On the other hand, intact IGFBP-5 protein was detected in the brain, pituitary gland, heart, stomach and kidney, while GAPDH was detected in all tissues tested by Western blot analysis (Supplementary Figure 2, Supporting Information). Judging from these results, the extent of IGFBP-5 processing to AMP-IBP5 was different in each tissue.

IR-AMP-IBP5 in rat brain extract was characterized by chromatographies. In gel filtration on a Sephadex G-50 column, IR-AMP-IBP5 occurred as a distinctive peak in the region of relative molecular mass less than 4 kDa (Figure 6A). Subsequently, we separated the IR-AMP-IBP5-rich fractions (Figure 6A, open box) using reverse phase HPLC and obtained two major peaks of IR-AMP-IBP5 (Figure 6B). The peak eluted earlier (Figure 6B, open arrow) behaved consistently with synthetic AMP-IBP5, while the peak eluted later remained unidentified. To identify the major endogenous molecular form, we analyzed the earlier eluted peak by MS of immunoprecipitates, and obtained a dominant peak at m/z 2654.3 ($[M + H]^+$ ion) (Figure 6C). This mass value corresponded to the theoretical mass of synthetic AMP-IBP5 (m/z, 2654.4), which was calculated as a disulfide-linked, C-terminally amidated peptide from rat IGFBP-5[193-214].

We characterized IR-AMP-IBP5 also in the small intestine extract. As in the brain extract, most immunoreactivity was observed less than 4 kDa in the gel filtration chromatography (Supplementary Figure 3A, Supporting Information) and separated into two major peaks of IR-AMP-IBP5 by reverse phase HPLC (Supplementary Figure 3B). The earlier eluted peak (Supplementary Figure 3B, open arrow, Supporting Information) was consistent with synthetic AMP-IBP5, as assessed by the retention time. MS

dx.doi.org/10.1021/pr101114a | J. Proteome Res. XXXX, XXX, 000–000